Michikawa M, Lee YS, Kang KS.	differentiation through activation of p38MAP kinase signaling.				
Byun K, Kim J, Cho SY, Hutchinson B, Yang SR, Kang KS, Cho M, Hwang K, Michikawa M, Jeon YW, Paik YK, Lee B.	Proteomics, 6(4):1230-1236 Alteration of the glutamate and GABA transporters in the hippocampus of the Niemann-Pick disease, type C mouse using proteomic analysis".	***Proteomics,***	6	1230-1236	2006
道川 誠	アルツハイマー病とコレステロール代謝	生化学	78 巻 (9 号)	831-839	2006
道川 誠	アルツハイマー病:ベッドサイドからベンチへ	医療	60 巻 (12 号)	752-759	2006
Ko M, Zou K, Minagawa H, Yu W, Gong JS, Yanagisawa K,and Michikawa M	Cholesterol-mediated neurite outgrowth is differently regulated between cortical and hippocampal neurons.	***J Biol Chem***	280	42759-42765	2005
Yu W, Gong J-S, Ko M, Garver W. S., Yanagisawa K, and Michikawa M.	Altered cholesterol metabolism in Niemann-Pick Type C1 mouse brain affects mitochondria function"	***J Biol Chem***	280	11731-11739	2005
Yu W, Ko M, Yanagisawa K, and Michikawa M	Neurodegeneration in heterozygous Niemann-Pick type C1 (NPC1) mouse: Implication of heterozygous NPC1 mutations being a risk for tauopathy.	***J Biol Chem***	280	27296-302	2005
Yu W, Zou K, Gong JS, Ko M, Yanagisawa K, and Michikawa M	Oligomerization of amyloid β-protein occurs during the isolation of lipid rafts.	***J Neurosci Res.***	80	114-119	2005
Kim MJ, Kim J, Michikawa M, Cha CI, Lee B.	Substance P immunoreactive cell reductions in cerebral	***Brain Res,***	1043	218-224,	2005

	cortex of Niemann-Pick diseasse type C mouse".				
Yang SR, Kim SJ, Byun KH, Hutchinson B, Lee HH, Michikawa M, Lee YS, Kang KS	NPC1 gene deficiency leads to lack of neural stem cell self-renewal and abnormal differentiation through activation of p38MAP kinase signaling	*Stem Cells*	24	292-298	2005
Byun K, Kim J, Cho SY, Hutchinson B, Yang SR, Kang KS, Cho M, Hwang K, Michikawa M, Jeon YW, Paik YK, Lee B.	Alteration of the glutamate and GABA transporters in the hippocampus of the Niemann-Pick disease, type C mouse using proteomic analysis"	*Proteomics*	6	1230-1236	2005
Okamura N, Furumoto S, Funaki Y, Suemoto T, Kato M, Ishikawa Y, Ito S, Akatsu H, Yamamoto T, Sawada T, Arai H, Kudo Y and Yanai K	Binding and safety profile of novel benzoxazole derivative for in vivo imaging of amyloid deposits in Alzheimer's disease	*Geriatrics & Gerontology International.*	27	393-400	2007
Wei, J. et al.	Enhanced lysosomal pathology caused by beta-synuclein mutants linked to dementia with Lewy bodies.	*J Biol Chem*	282	28904-14	2007
Waragai, M. et al.	Plasma levels of DJ-1 as a possible marker for progression of sporadic Parkinson's disease	*Neurosci Lett*	425	18-22	2007
Nakai, M. et al.	Expression of alpha-synuclein, a presynaptic protein implicated in Parkinson's disease, in erythropoietic lineage.	*Biochem Biophys Res Commun*	358	104-10	2007
Makino, S. et al.	Reduced neuron-specific expression of the TAF1 gene is associated with	*Am J Hum Genet*	80,	393-406	2007

	X-linked dystonia-parkinsonism.				
Kimura, R. et al.	The DYRK1A gene, encoded in chromosome 21 Down syndrome critical region, bridges between beta-amyloid production and tau phosphorylation in Alzheimer disease.	***Hum Mol Genet***	**16,.**	15-23	2007
Kanai, Y., Akatsu, H., Iizuka, H. & Morimoto, C.	Could serum antibody to poly(ADP-ribose) and/or histone H1 be marker for senile dementia of Alzheimer type?	***Ann N Y Acad Sci***	**1109,**	338-44	2007
Akatsu, H. et al.	Plasma levels of unactivated thrombin activatable fibrinolysis inhibitor (TAFI) are down-regulated in young adult women: analysis of a normal Japanese population.	***Microbiol Immunol***	**51,**	507-17	2007
Yokota, T. et al.	Brain site-specific gene expression analysis in Alzheimer's disease patients.	***Eur J Clin Invest***	**36,**	820-30	2006
Waragai, M. et al.	Increased level of DJ-1 in the cerebrospinal fluids of sporadic Parkinson's disease.	***Biochem Biophys Res Commun***	**345,**	967-72	2006
Mitsuda, N. et al.	A novel alternative splice variant of nicastrin and its implication in Alzheimer disease.	***Life Sci***	**78,**	2444-8	2006
Satoh K, et al .	A novel membrane protein, encoded by the gene covering KIAA0233, is transcriptionally induced in senile plaque-associated astrocytes.	***Brain Res.***	**1108,**	19-27	2006
Kimura, R. et al.	Albumin gene encoding free fatty acid and beta-amyloid transporter is genetically associated	***Psychiatry Clin Neurosci***	**60**	**Suppl 1,** S34-9	2006

	with Alzheimer disease.				
Isojima, D. et al.	Vascular complications in dementia with Lewy bodies: a postmortem study.	*Neuropathology*	**26,**	293-7	2006
Heese, K. & Akatsu, H.	Alzheimer's disease--an interactive perspective.	*Curr Alzheimer Res*	**3,**	109-21	2006
Fujishiro, H. et al.	Depletion of cholinergic neurons in the nucleus of the medial septum and the vertical limb of the diagonal band in dementia with Lewy bodies.	*Acta Neuropathol*	**111,**	109-14	2006
Akatsu, H. et al.	Variations in the BDNF gene in autopsy-confirmed Alzheimer's disease and dementia with Lewy bodies in Japan.	*Dement Geriatr Cogn Disord*	**22,**	216-22	2006
Zhong, W. et al.	Lymphocyte-specific protein tyrosine kinase is a novel risk gene for Alzheimer disease.	*J Neurol Sci*	**238,**	53-7	2005
Yamamoto, R. et al.	Non-uniformity in the regional pattern of Lewy pathology in brains of dementia with Lewy bodies.	*Neuropathology*	**25,**	188-94	2005
Togo, T. et al.	Clinical features of argyrophilic grain disease: a retrospective survey of cases with neuropsychiatric symptoms.	*Am J Geriatr Psychiatry*	**13,**	1083-91	2005
Taguchi, K. et al.	Identification of hippocampus-related candidate genes for Alzheimer's disease.	*Ann Neurol*	**57,**	585-8	2005
Satoh, K. et al.	Lib, transcriptionally induced in senile plaque-associated astrocytes, promotes glial migration through extracellular matrix.	*Biochem Biophys Res Commun*	**335,**	631-6	2005
Okamura, N. et al.	Quinoline and benzimidazole	*J Neurosci*	**25,**	10857-62	2005

	derivatives: candidate probes for in vivo imaging of tau pathology in Alzheimer's disease.				
Kanie, J., Akatsu, H. & Suzuki, Y.	A case of misinsertion of the PEG tube into the abdominal cavity recovered on a referral to the outpatient by using simple endoscopy techniques.	***Nippon Ronen Igakkai Zasshi***	**42,**	698-701	2005
Iwasaki T., Takahashi S., Takahashi M., Zenimaru Y., Kujiraoka T., Ishihara M., Nagano M., Suzuki J., Miyamori I., Naiki H., Sakai J., Fujino T., Norman E. Miller N. E., Yamamoto T. T. and Hattori H..	Deficiency of the very low-density lipoprotein (vldl) receptors in streptozotocin-induce d diabetic rats: insulin-dependency of the vldl receptor.	***Endocrinology***	146,	3286-329 4	2005

III. 研究成果の刊行物・別刷

Neurobiology of Disease

Angiotensin-Converting Enzyme Converts Amyloid β-Protein 1–42 ($A\beta_{1-42}$) to $A\beta_{1-40}$, and Its Inhibition Enhances Brain Aβ Deposition

Kun Zou,[1,3] Haruyasu Yamaguchi,[4] Hiroyasu Akatsu,[5] Takaaki Sakamoto,[1] Mihee Ko,[1] Kazushige Mizoguchi,[2] Jian-Sheng Gong,[1] Wenxin Yu,[1] Takayuki Yamamoto,[5] Kenji Kosaka,[5] Katsuhiko Yanagisawa,[1] and Makoto Michikawa[1]

Departments of [1]Alzheimer's Disease Research and [2]Geriatric Medicine, National Institute for Longevity Sciences, National Center for Geriatrics and Gerontology, Obu, Aichi 474-8522, Japan, [3]Japan Society for the Promotion of Science, Tokyo 102-8471, Japan, [4]Gunma University School of Health Sciences, Maebashi 371-8514, Japan, and [5]Choju Medical Institute, Fukushimura Hospital, Toyohashi 441-8124, Japan

The abnormal deposition of the amyloid β-protein (Aβ) in the brain appears crucial to the pathogenesis of Alzheimer's disease (AD). Recent studies have suggested that highly amyloidogenic $A\beta_{1-42}$ is a cause of neuronal damage leading to AD pathogenesis and that monomeric $A\beta_{1-40}$ has less neurotoxicity than $A\beta_{1-42}$. We found that mouse and human brain homogenates exhibit an enzyme activity converting $A\beta_{1-42}$ to $A\beta_{1-40}$ and that the major part of this converting activity is mediated by the angiotensin-converting enzyme (ACE). Purified human ACE converts $A\beta_{1-42}$ to $A\beta_{1-40}$ as well as decreases $A\beta_{1-42}/A\beta_{1-40}$ ratio and degrades $A\beta_{1-42}$ and $A\beta_{1-40}$. Importantly, the treatment of Tg2576 mice with an ACE inhibitor, captopril, promotes predominant $A\beta_{1-42}$ deposition in the brain, suggesting that ACE regulates $A\beta_{1-42}/A\beta_{1-40}$ ratio *in vivo* by converting secreted $A\beta_{1-42}$ to $A\beta_{1-40}$ and degrading Aβs. The upregulation of ACE activity can be a novel therapeutic strategy for AD.

Key words: angiotensin-converting enzyme; ACE; Alzheimer's disease; amyloid β-protein; Aβ; Aβ deposition; Aβ degradation; APP transgenic mouse

Introduction

The progressive accumulation and deposition of the amyloid β-protein (Aβ) in the brain are early pathogenically important features of Alzheimer's disease (AD) (Selkoe, 2004). It has been assumed that insoluble Aβ amyloid is a culprit for inducing the pathological processes of AD, leading to neuronal dysfunction; however, recent studies have shown that not the insoluble form of Aβ but the soluble form of Aβ oligomers is pathogenic (Kirkitadze et al., 2002; Walsh et al., 2002). $A\beta_{1-42}$ is deposited early and selectively in senile plaques, and this deposition is an invariant feature of all forms of AD (Iwatsubo et al., 1994). A high $A\beta_{42}/A\beta_{40}$ ratio is a major determinant for AD development in familial AD with presenilin mutations (Borchelt et al., 1996; Duff et al., 1996; Scheuner et al., 1996; Citron et al., 1997).

Aβs ($A\beta_{1-40}$ and $A\beta_{1-42}$) are constantly secreted by many types of cell and are normally found in body fluids, including CSF. Recently, we have shown that monomeric $A\beta_{1-40}$ has neuroprotective effects against metal-induced oxidative damage and $A\beta_{1-42}$-induced neuronal death, whereas $A\beta_{1-42}$ is highly amyloidogenic and thus forms oligomers rapidly at very low concentrations, exerting strong neurotoxicity (Zou et al., 2002, 2003). $A\beta_{1-40}$, but not $A\beta_{1-42}$, rescues neurons from β- or γ-secretase inhibitor-induced cell death (Plant et al., 2003). Moreover, the inhibition of the effects of some nonsteroidal anti-inflammatory drugs, which reduce the risk of AD (in 't Veld et al., 2001), directly blocks $A\beta_{1-42}$ generation by changing presenilin conformation and shifting γ-secretase function toward the production of a shorter soluble Aβ (Weggen et al., 2001; Lleo et al., 2004).

A recent study demonstrated that $A\beta_{42}$ is essential for parenchymal and vascular amyloid deposition in mice and that mice expressing a high $A\beta_{1-40}$ level do not develop overt amyloid pathology (McGowan et al., 2005). Both $A\beta_{1-42}$ and $A\beta_{1-40}$ levels were elevated coordinately in late-onset sporadic AD brains (Selkoe, 2004) and non-AD human brains (Morishima-Kawashima et al., 2000); however, insoluble $A\beta_{42}$ level increases exponentially and steeply in an age-dependent manner, accompanied by much smaller increases in $A\beta_{40}$ level (Morishima-Kawashima et al., 2000). Thus, although it is still debatable whether $A\beta_{1-40}$ is nontoxic or neuroprotective, these findings suggest that decreasing neurotoxic $A\beta_{1-42}$ level could be a strategy for developing AD treatments.

We considered that there is a carboxyl peptidase that converts

Received Dec. 23, 2006; revised June 11, 2007; accepted June 29, 2007.

This work was supported by grants from the Ministry of Health, Labor, and Welfare of Japan (Research on Human Genome and Tissue Engineering Grant H17-004), the Program for Promotion of Fundamental Studies in Health of the National Institute of Biomedical Innovation, and Japan Society for the Promotion of Science, and Grant-in-Aid 18023046 for Scientific Research on Priority Areas-Research on Pathomechanisms of Brain Disorders from the Ministry of Education, Culture, Sports, Science, and Technology of Japan.

Correspondence should be addressed to Dr. Makoto Michikawa, Department of Alzheimer's Disease Research, National Institute for Longevity Sciences, National Center for Geriatrics and Gerontology, 36-3 Gengo, Morioka, Obu, Aichi 474-8522, Japan. E-mail: michi@nils.go.jp.

K. Zou's present address: Department of Neuroscience, Faculty of Pharmaceutical Sciences, Iwate Medical University, Yahaba 028-3694, Japan.

DOI:10.1523/JNEUROSCI.1549-07.2007

 0270-6474/07/278628-08$15.00/0

secreted neurotoxic $A\beta_{1-42}$ to $A\beta_{1-40}$, thus decreasing $A\beta_{42}/A\beta_{40}$ ratio. This notion has led us to experimentally identify an $A\beta_{1-42}$-to-$A\beta_{1-40}$-converting enzyme in the mouse and human brains. Interestingly, we found that the angiotensin-converting enzyme (ACE) is a major $A\beta_{1-42}$-to-$A\beta_{1-40}$-converting enzyme in the brain. This suggests that the modulation of ACE activity can be a novel therapeutic strategy for AD.

Materials and Methods

Captopril treatment of Tg2576 mice and tissue preparation. Male human amyloid precursor protein Swedish mutation (hAPPsw) transgenic Tg2576 mice were purchased from Taconic Farms (Germantown, NY). Mice at 6 months of age were fed with captopril-supplemented diet (0.25 mg/g) or control diet *ad libitum* for 7 or 11 months. There were 6–15 animals in each group. Animals were housed singly in individual cages. There were no significant differences in the amount of feed consumed or in the weight of the mice within or between treatment groups. The average captopril intake per animal was 30 mg/kg of body weight/d. Mice were killed by inhalation of CO_2, and 0.5 ml of blood was collected from the right atrium for the determination of serum ACE activity. Mice were then transcardially perfused with cold PBS. The left hemisphere of the brain was fixed in 4% buffered paraformaldehyde solution at 4°C for 48 h and incubated in 30% sucrose at 4°C for 48 h for histological processing. The right hemisphere of the brain was separated into the cerebral cortex, hippocampus, thalamus, and brainstem, and these samples were rapidly frozen in liquid nitrogen and stored at −80°C until analysis.

Human postmortem brain tissue. Frontal cortex tissue samples from autopsied control subjects ($n = 15$; male, 9, female, 6; neuropathological diagnosis, physiological aging) and AD subjects ($n = 15$; male, 9, female, 6; clinical and neuropathological diagnosis, AD) were obtained from Fukushimura Hospital (Toyohashi, Japan). Tissues were frozen immediately in liquid nitrogen at autopsy and then stored at −80°C until use. The average postmortem delay was 7.7 h and was not significantly different between the two groups. The average age of the subjects of the control group was 84.7 ± 1.9, and that of the subjects of the AD group was 85.5 ± 1.9 (data represent means ± SEM; $p = 0.75$, ANOVA, Bonferroni/Dunn test). Experiments using human brains were performed after obtaining the informed consent of the patients' guardians for diagnosis and biochemical, molecular biological, and genomic research. This study was examined and approved by the Ethics Committee of Fukushimura Hospital on October 6, 2005, and assigned the application number 180.

ACE activity assay. Cortical tissue (50–100 mg) was homogenized in a fourfold (w/v) volume of ACE homogenization buffer (50 mM HEPES, pH 7.4, 150 mM NaCl, 25 μM $ZnCl_2$, and 0.5% Triton X-100) and centrifuged at 4°C at 10,000 × *g* for 15 min. ACE activity in the supernatant against the synthetic substrate *N*-hippuryl-l-histidyl-l-leucine was determined using an ACE colorimetric kit (Buhlmann Laboratories, Schonenbuch, Switzerland). The reaction time was 6 h. ACE activity was then normalized by the initial weight of the brain tissue. For mouse serum ACE activity assay, serum was diluted at 1:2. All samples were measured in triplicate.

Western blot analysis for determining conversion of $A\beta_{1-42}$ to $A\beta_{1-40}$. Somatic ACE-deficient mice (002680) were obtained from The Jackson Laboratory (Bar Harbor, ME). $A\beta_{1-42}$ (Peptide Institute, Osaka, Japan) was freshly dissolved in 0.1% $NH_3.H_2O$ at 200 μM for each experiment. The wild-type mouse brain cortex, including the hippocampus, was homogenized in a twofold volume (w/v) of a buffer containing 10 mM Tris.HCl, pH 7.5, and 0.15 M NaCl, and the homogenate was centrifuged at 500 × *g* for 10 min. The supernatant was mixed with synthetic $A\beta_{1-42}$ to a final concentration of 30 μM and incubated at 37°C for 8 h. Ten microliters of the mixture was subjected to SDS-PAGE and blotted on a nitrocellulose membrane. To enhance the reactivity to an anti-$A\beta_{1-40}$ antibody, the membrane was boiled in PBS for 3 min after blotting, probed with an anti-$A\beta_{1-40}$ monoclonal antibody (1A10) (IBL, Takasaki, Japan), and visualized with SuperSignal (Pierce, Rockford, IL). Because of the high level of exogenous $A\beta_{1-42}$, the membrane was not boiled before the reaction with a polyclonal anti-$A\beta_{1-42}$ antibody.

Thioflavin-T binding assay for aggregated Aβ. Determination of the aggregated state of Aβ was performed on the basis of a previously established method (Levine, 1995, 1999). The incubated Aβ peptides were centrifuged at 17,000 × *g* for 60 min, the supernatant was removed, and the precipitate was suspended in 1 ml of 5 μM thioflavin-T in 50 mM glycine-NaOH, pH 8.5. Steady-state fluorescence intensities for each sample were determined as described previously (Zou et al., 2002).

Matrix-assisted laser desorption ionization-time of flight mass spectrometry. Purified human ACE (2 U/ml) (Millipore, Billerica, MA) was added to 30 μM $A\beta_{1-42}$ dissolved in 0.1% $NH_3.H_2O$ and incubated at 37°C for 6 h. Captopril (2 mM) was added to stop the digestion, and the sample was frozen in −80°C until use. The sample was subjected to matrix-assisted laser desorption/ionization-time of flight mass spectrometry (MALDI-TOF-MS) to detect the generation of $A\beta_{1-40}$. The same amount of ACE or $A\beta_{1-42}$ incubated alone under the same conditions as described above was used as control.

Biotinylation of $A\beta_{1-42}$ and determination of $A\beta_{1-42}$-to-$A\beta_{1-40}$-converting activity in human brain. $A\beta_{1-42}$ was biotinylated using a ProtOn biotin labeling kit (Vector Laboratories, Burlingame, CA). In brief, 0.5 mg of $A\beta_{1-42}$ was dissolved in DMSO and diluted with distilled water to 100 μl. $A\beta_{1-42}$ was biotinylated with a biotin-labeling reagent, and free biotin was removed using gel filtration slurry provided with the kit. The human frontal cortex tissue sample used was from a 76-year-old autopsied non-AD subject. The brain tissue was homogenized in a fourfold volume (w/v) of PBS, and the homogenate was mixed with biotinylated $A\beta_{1-42}$ at a concentration of 0.5 μg/μl. The mixtures were incubated at 37°C for 8 h with or without an ACE inhibitor (1 μM), namely captopril or enalapril. After incubation, 8 mM 3-[(3-cholamidopropyl)dimethylammonio]-1-propanesulfonate was added to extract Aβs. The samples were centrifuged at 4°C and 10,000 × *g* for 10 min, and the supernatant was applied to avidin agarose provided with the kit to purify biotinylated Aβs. Avidin agarose was washed with PBS four times, and biotinylated Aβs were eluted with 50 mM DTT in SDS-PAGE sample buffer. Biotinylated $A\beta_{1-40}$ converted from biotinylated $A\beta_{1-42}$ was detected by Western blot analysis using an anti-$A\beta_{1-40}$ monoclonal antibody (1A10).

Immunohistochemistry. The left hemispheres of the brains of Tg2576 mice were sagittally cut into 30 μm sections using a freezing microtome (RM 2145; Leica, Wetzlar, Germany). Thioflavin-S staining was performed as described previously (Wyss-Coray et al., 2001). For each mouse, thioflavin-S-positive plaques were counted in four to five sections per left hemisphere of the brain at a magnification of 40×. Serial sections were immunostained with anti-$A\beta_{1-40}$ and anti-$A\beta_{1-42}$ end-specific polyclonal antibodies, namely, RIB40 and RIB42, respectively (2 μg/ml; IBL), after a brief formic acid pretreatment, and immunopositive signals were visualized using an ABC elite kit (Vector Laboratories). Images of the cerebral cortex and hippocampus were captured using a digital camera attached to a microscope and analyzed using simple PCI software (Compix Imaging Systems, Lake Oswego, OR). $A\beta_{1-40}$ and $A\beta_{1-42}$ plaques were estimated as the percentage of immunostained area (positive pixels) divided by the examined area (total pixels). The quantification of thioflavin-S-positive plaques and areas attained by anti-$A\beta_{1-40}$ and anti-$A\beta_{1-42}$ antibodies was performed in a double-blind manner.

Aβ ELISA. Mouse cortices for ELISA were homogenized in 10 volumes of a mixture containing 5.0 M guanidine.HCl and 50 mM Tris.HCl, pH 8.0 (w/v), as described previously (Johnson-Wood et al., 1997). The brain homogenates were further diluted at 1:20 for 13-month-old and 1:500 for 17-month-old mice in a dilution buffer provided with the ELISA kit (Wako, Osaka, Japan). $A\beta_{1-42}$ and $A\beta_{1-40}$ standards (Peptide Institute) were prepared such that the final composition included the same concentration of guanidine. Purified human ACE (2 U/ml) with 10 μM $A\beta_{1-42}$ was diluted at 1:1000 with a dilution buffer containing complete protease inhibitor mixture (Roche, Mannheim, Germany). $A\beta_{1-42}$ and $A\beta_{1-40}$ levels were determined using the ELISA kit. Fibroblasts stably expressing human APP695 (Shiraishi et al., 2004) were grown in DMEM (Invitrogen, Grand Island, NY) containing 10% fetal calf serum. The medium was changed at 100% confluence, and the fibroblasts were treated with or without captopril. The levels of $A\beta_{1-40}$ and $A\beta_{1-42}$ in the medium were determined 24 h after the treatment of fibroblasts with captopril. All samples were measured in triplicate.

Results

We used two specific anti-$A\beta_{1-42}$ and anti-$A\beta_{1-40}$ antibodies to examine $A\beta_{1-40}$ generation in a tissue homogenate mixed with exogenously added synthetic $A\beta_{1-42}$. There was no cross-reaction between the two antibodies, which was confirmed by Western blot analysis (Fig. 1*A*). The coincubation of $A\beta_{1-42}$ with mouse cerebral homogenate generated $A\beta_{1-40}$, indicating the existence of an $A\beta_{1-42}$-to-$A\beta_{1-40}$-converting enzyme. Also, the generation of $A\beta_{1-40}$ from synthetic $A\beta_{1-42}$ was inhibited by the ACE inhibitors captopril and enalapril (Fig. 1*B*; supplemental Table 1, available at www.jneurosci.org as supplemental material). This converting activity was also found in the mouse cerebellum, kidney, heart, spleen, lung, skeletal muscle, and serum, indicating that the $A\beta_{1-42}$-to-$A\beta_{1-40}$-converting enzyme is distributed widely. In our Western blot system, neither endogenous $A\beta_{1-40}$ nor $A\beta_{1-42}$ was detected in these samples (data not shown). Moreover, Western blot analysis showed that the brain homogenate and serum from somatic ACE-deficient mice contain a markedly decreased capacity of generating $A\beta_{1-40}$ from $A\beta_{1-42}$ compared with those from wild-type (ACE+/+) and heterozygote (ACE+/−) mice (Fig. 1*C*). ACE is a dipeptidyl carboxypeptidase that catalyzes the cleavage of C-terminal dipeptides of several substrates and is widely distributed in mammalian tissues. These lines of evidence suggest that ACE in the brain homogenate plays a major role in the conversion of $A\beta_{1-42}$ to $A\beta_{1-40}$.

Thus, we next performed Western blot analysis, ELISA, and MALDI-TOF-MS to examine whether purified human ACE cleaves the 2 aa at the C terminus of synthetic $A\beta_{1-42}$ to generate $A\beta_{1-40}$. After the incubation of $A\beta_{1-42}$ with ACE, $A\beta_{1-40}$ level increased in a time-dependent manner, whereas $A\beta_{1-42}$ level decreased (Fig. 1*D*,*G*). Determination of the level of $A\beta_{1-40}$ generated and $A\beta_{1-42}$ remaining in the solution containing synthetic $A\beta_{1-42}$ and ACE shows that the levels of $A\beta_{1-40}$ and $A\beta_{1-42}$ were inversely and significantly correlated (supplemental Fig. 1*C*, available at www.jneurosci.org as supplemental material). $A\beta_{1-40}$ generation was completely inhibited by ACE inhibitors, namely, EDTA, captopril, and enalapril (Fig. 1*D*; supplemental Table 2, available at www.jneurosci.org as supplemental material). Because $A\beta_{1-42}$ can easily aggregate in aqueous buffers, it is important to understand whether ACE can mediate the cleavage of the aggregated form of $A\beta_{1-42}$. We performed thioflavin-T assay to monitor $A\beta_{1-42}$ aggregation. The thioflavin-T fluorescence of $A\beta_{1-42}$ incubated with or without ACE or of the mouse brain lysate showed no increase after 8 h of incubation. After 24 h of incubation, the thioflavin-T fluorescence of $A\beta_{1-42}$ incubated alone and with the brain homogenate markedly increased; however, ACE strongly inhibited the increase in thioflavin-T fluorescence (supplemental Fig. 1*A*, available at www.jneurosci.org as supplemental material). These results suggest that $A\beta_{1-40}$ is converted from nonfibril $A\beta_{1-42}$ within 8 h of incubation. We previously reported that $A\beta_{1-42}$ with random structures transformed to a β-sheet structure after 4 h of incubation at 37°C (Zou et al., 2003). Together with the present finding that the level of $A\beta_{1-40}$ converted from $A\beta_{1-42}$ increased until 8 h of incubation, it is possible that ACE generates $A\beta_{1-40}$ from $A\beta_{1-42}$ with both random and β-sheet structures.

Next we examined whether ACE degrades or converts aggregated $A\beta_{1-42}$. ACE did not reduce the thioflavin-T fluorescence of aggregated $A\beta_{1-42}$ after 24 h of incubation (supplemental Fig. 1*B*, available at www.jneurosci.org as supplemental material), and no $A\beta_{1-40}$ converted from $A\beta_{1-42}$ was detected by Western

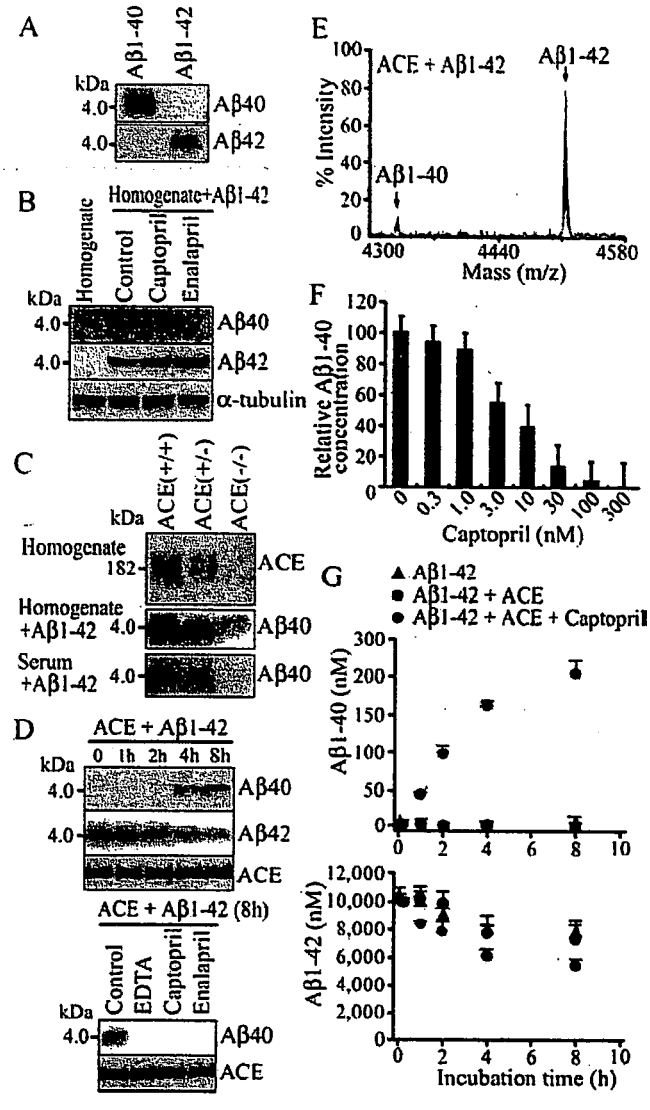

Figure 1. ACE converts $A\beta_{1-42}$ to $A\beta_{1-40}$. *A*, We confirmed the specificities of monoclonal anti-$A\beta_{1-40}$ (1A10) and polyclonal anti-$A\beta_{1-42}$ antibodies. One microgram each of $A\beta_{1-40}$ and $A\beta_{1-42}$ was subjected to SDS-PAGE and then blotted onto a nitrocellulose membrane, and the membrane was probed with anti-$A\beta_{1-40}$ and anti-$A\beta_{1-42}$ antibodies. *B*, Mouse brain homogenate was mixed with or without synthetic $A\beta_{1-42}$ and incubated at 37°C for 8 h. An anti-$A\beta_{1-40}$ antibody was used for detecting $A\beta_{1-40}$ generation. Captopril (1 μM) or enalapril (1 μM) markedly inhibited the generation of $A\beta_{1-40}$ from $A\beta_{1-42}$. *C*, Top, The genotypes of ACE(+/+), ACE(+/−), and ACE(−/−) mice were confirmed by Western blot analysis of the brain homogenate using an anti-ACE polyclonal antibody (AF1513; R & D Systems). Middle, Bottom, Mouse brain homogenate (middle) or serum (bottom) was mixed with 30 μM $A\beta_{1-42}$ and incubated at 37°C for 8 h. The generation of $A\beta_{1-40}$ was detected by Western blot analysis. *D*, Purified human ACE (2 U/ml) was mixed with synthetic $A\beta_{1-42}$ (30 μM), and the mixture was incubated at 37°C with or without ACE inhibitors. Top, $A\beta_{1-40}$ was generated in a time-dependent manner. Bottom, EDTA (10 μM), captopril (1 μM), and enalapril (1 μM) completely inhibited the conversion of $A\beta_{1-42}$ to $A\beta_{1-40}$. *E*, MALDI-TOF-MS revealed a new peak with a mass of 4330 (corresponding to that of $A\beta_{1-40}$) after the incubation of $A\beta_{1-42}$ with ACE, indicating $A\beta_{1-40}$ generation. *F*, Captopril blocked $A\beta_{1-40}$ generation in the mixture of $A\beta_{1-42}$ and purified human ACE in a dose-dependent manner. The density of $A\beta_{1-40}$ bands was measured by densitometry and normalized to the mean of the bands in the case of incubation without captopril. IC_{50} was estimated to be ~10 nM. *G*, Time-dependent alterations in $A\beta_{1-42}$ and $A\beta_{1-40}$ levels in the solution of $A\beta_{1-42}$ (10 μM) alone; $A\beta_{1-42}$ (10 μM) and ACE (2 U/ml); or $A\beta_{1-42}$ (10 μM), ACE (2 U/ml), and captopril (1 μM). Each solution was incubated at 37°C for the time indicated. Ten microliters of each solution were collected at different time points and immediately frozen at −80°C until analysis. The levels of $A\beta_{1-42}$ and $A\beta_{1-40}$ in each sample were determined by ELISA. Data are the mean ± SEM of three samples.

Table 1. Kinetic parameters for conversion of Aβ1–42 to Aβ1–40 by human kidney ACE

Substrate	Product	K_m (μM)	k_{cat} (s^{-1})	k_{cat}/K_m ($s^{-1}\cdot mM^{-1}$)
$A\beta_{1-42}$	$A\beta_{1-40}$	7	4.2	600

$A\beta_{1-42}$ peptides (0, 2.5, 5, 10, 15, 20, 25, 30, and 50 μM) were incubated at 37°C for 8 h with human kidney ACE (0.45 μM). The level of $A\beta_{1-40}$ was determined by ELISA, and K_m, k_{cat}, and k_{cat}/K_m were then calculated.

blot analysis (data not shown), suggesting that ACE cannot degrade aggregated $A\beta_{1-42}$ or convert aggregated $A\beta_{1-42}$ to $A\beta_{1-40}$. MALDI-TOF-MS demonstrated peaks with molecular masses of 4330 and 4514 after incubation for 8 h, which matched the predicted masses of $A\beta_{1-40}$ and $A\beta_{1-42}$, respectively (Fig. 1*E*). MALDI-TOF-MS of the reaction mixture of ACE and $A\beta_{1-42}$ revealed several peaks with masses corresponding to those of $A\beta_{1-35}$, $A\beta_{1-34}$, $A\beta_{1-22}$, $A\beta_{1-20}$, and $A\beta_{1-19}$, in addition to $A\beta_{1-40}$. Interestingly, however, no $A\beta_{1-38}$, $A\beta_{1-7}$, or $A\beta_{8-42}$ was detected by our MALDI-TOF-MS. No $A\beta_{1-40}$ was detected by MALDI-TOF-MS in a solution of purified ACE or synthetic $A\beta_{1-42}$ after incubation at 37°C (supplemental Fig. 2, available at www.jneurosci.org as supplemental material). The IC_{50} of captopril needed for purified human ACE to convert $A\beta_{1-42}$ to $A\beta_{1-40}$ was ~10 nM, indicating the specific inhibitory effect of captopril on ACE-mediated $A\beta_{1-42}$-to-$A\beta_{1-40}$ conversion (Fig. 1*E*).

Next we determined the level of $A\beta_{1-40}$ converted from $A\beta_{1-42}$ and that of $A\beta_{1-42}$ remaining in the mixture of $A\beta_{1-42}$ and ACE using an ELISA kit. To determine the level of $A\beta_{1-42}$ lost from the solutions as a result of the "sticky" nature of $A\beta_{1-42}$, we also determined $A\beta_{1-42}$ level in the absence or presence of ACE with an ACE inhibitor as control. During the incubation of $A\beta_{1-42}$ with ACE for 2–8 h, ~10–20% of the degraded $A\beta_{1-42}$ was converted to $A\beta_{1-40}$. These results indicate that $A\beta_{1-40}$ can be generated from $A\beta_{1-42}$ through the action of ACE and that ACE cleaves $A\beta_{1-42}$ at other sites as well (Fig. 1*F*), which are supported by the results of MALDI-TOF-MS. Moreover, $A\beta_{40}/A\beta_{42}$ ratio increased during the incubation period, suggesting that ACE decreases $A\beta_{42}/A\beta_{40}$ ratio via its $A\beta_{1-42}$-to-$A\beta_{1-40}$-converting activity (data not shown). To understand the catalytic efficiency of ACE converting $A\beta_{1-42}$ to $A\beta_{1-40}$, we performed a kinetic assay of this conversion. The K_m, k_{cat}, and k_{cat}/K_m of the $A\beta_{1-42}$-to-$A\beta_{1-40}$ conversion by ACE were determined to be 7 μM, 4.2 s^{-1}, and 600 $s^{-1}\cdot mM^{-1}$, respectively (Table 1). These values were similar to those of ACE for angiotensin I (Ang I) hydrolysis (Hayakari et al., 2003). Thus, this $A\beta_{1-42}$-to-$A\beta_{1-40}$ conversion activity of ACE is likely favorable *in vivo* under normal physiological conditions.

To determine whether the human brain shows this $A\beta_{1-42}$-to-$A\beta_{1-40}$-converting activity and whether the activity is inhibited by ACE inhibitors, we used the frontal cortex from a 76-year-old non-AD subject. To exclude the effect of endogenous $A\beta_{1-40}$, we labeled synthetic $A\beta_{1-42}$ with biotin. The sites of biotinylation were at lysine residues amino acid positions 16 and 28 in $A\beta_{1-42}$. The biotinylated Aβs were purified with avidin agarose, and biotinylated $A\beta_{1-40}$ generated from biotinylated $A\beta_{1-42}$ was detected by Western blot analysis. Similar to the results for the mouse brain homogenate, the incubation of $A\beta_{1-42}$ with the human brain homogenate resulted in the generation of $A\beta_{1-40}$, and this generation was inhibited by an ACE inhibitor, namely captopril or enalapril (Fig. 2*A*; supplemental Table 3, available at www.jneurosci.org as supplemental material). No endogenous $A\beta_{1-40}$ was detected in the human brain homogenate that was incubated without biotinylated $A\beta_{1-42}$ (Fig. 2*A*). These results indicate that the human brain also shows $A\beta_{1-42}$-to-$A\beta_{1-40}$-converting activity and that this activity is mainly mediated by ACE. To determine whether ACE activity and ACE expression level are altered in AD brains, we measured ACE activity and determined ACE expression level by Western blot analysis. AD brains showed reduced ACE activity and expression level compared with age-matched non-AD brains (Fig. 2*B–D*).

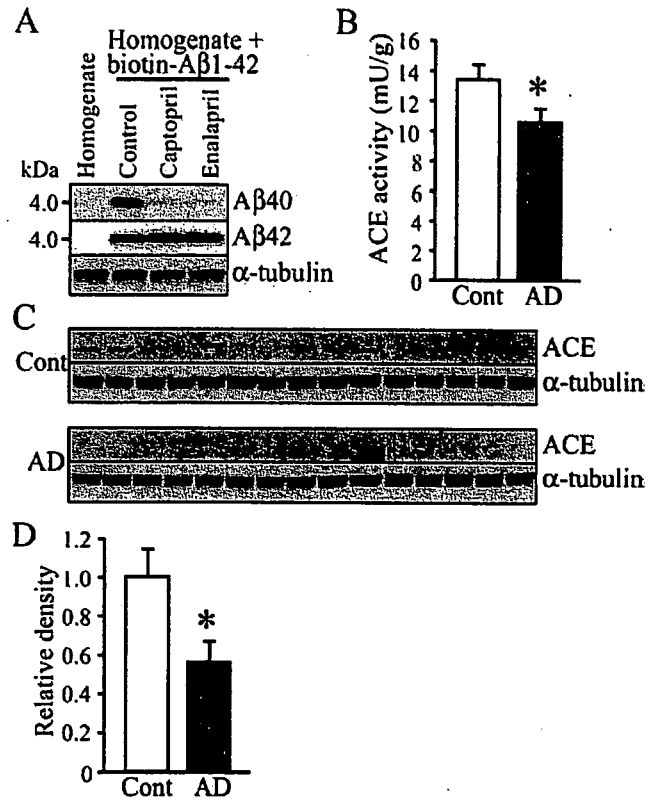

Figure 2. The human brain shows $A\beta_{1-42}$-to-$A\beta_{1-40}$-converting activity, and this ACE activity decreases in AD brain. ***A***, The frontal cortex from a non-AD subject was homogenized in PBS. Biotinylated $A\beta_{1-42}$ was added to the resulting homogenate, and the mixture was incubated at 37°C for 8 h with or without 1 μM ACE inhibitor, namely captopril or enalapril. Biotinylated Aβs were then purified using avidin agarose, and the conversion of $A\beta_{1-42}$ to $A\beta_{1-40}$ was detected by Western blot analysis using an anti-$A\beta_{1-40}$ monoclonal antibody (1A10) and an anti-$A\beta_{1-42}$ polyclonal antibody. ***B***, The cortices from the frontal gyri of the non-AD subjects and AD patients were homogenized in a lysis buffer. The resulting homogenate was centrifuged, and ACE activity in the supernatant was determined using an ACE colorimetric kit. The ACE activities of 15 non-AD control individuals (Cont) and 15 AD patients were measured. ***C***, The ACE expression level in the frontal cortex of those 30 subjects was determined by Western blot analysis, and a representative image is shown. Twenty micrograms of protein from the brain homogenate were subjected to SDS-PAGE and Western blot analysis. The membrane was probed with an anti-ACE polyclonal antibody. ***D***, The relative densities of the ACE bands were determined by densitometry. AD cases exhibited a significantly decreased ACE expression level. Data are the mean ± SEM of 15 samples. $^*p < 0.05$ versus non-AD control by Mann–Whitney *U* test.

To determine whether ACE inhibition promotes AD pathology, we administered captopril, a blood–brain barrier-penetrating ACE inhibitor, to an AD mouse model (hAPPsw, Tg2576) (Hsiao et al., 1996) and assessed its effect on brain amyloid deposition. Tg2576 mice were fed with a captopril-supplemented diet (captopril, 30 mg/kg of body weight/d) from 6 months of age. The mice were killed at 13 and 17 months of age, and their brains were analyzed. In the 13-month-old mice, captopril treatment resulted in a trend toward an increase in the number of thioflavin-S-positive plaques ($n = 6$ per group; control neocortex, 27.9 ± 6.3; neocortex of captopril-treated mice, 34.9 ± 7.3; $p = 0.8728$; control hippocampus, 11.3 ± 3.2; hip-

pocampus of captopril-treated mice, 21.3 ± 5.8; $p = 0.2623$, Mann–Whitney U test). Interestingly, the ELISA of Aβs demonstrated a significantly higher $A\beta_{1-42}$ level in the neocortex of the 13-month-old captopril-treated mice than in that of the control mice (control, 504.6 ± 14.1 pmol/g; captopril-treated mice, 643.7 ± 49.0 pmol/g; $p = 0.0374$); however, the level of $A\beta_{1-40}$ remained unchanged (control, 1690.2 ± 141.4 pmol/g; captopril-treated mice, 1700.0 ± 249.8 pmol/g; $p = 0.9361$, Mann–Whitney U test). These results suggest that captopril treatment enhances $A\beta_{1-42}$ deposition to a greater extent than $A\beta_{1-40}$ deposition in the brain.

The analysis of the 17-month-old captopril-treated mice showed 2.5-fold and twofold increases in the number of thioflavin-S-positive plaques in the cortex and hippocampus, respectively, compared with that of the control mice (Fig. 3*B*,*G*). Moreover, $A\beta_{1-42}$-immunopositive areas in the neocortex and hippocampus were respectively 2.6-fold and twofold larger in the 17-month-old captopril-treated mice than in the control mice (Fig. 3*A*,*C*,*H*). Captopril treatment resulted in an increase in $A\beta_{1-40}$-immunopositive area; however, the increase was not statistically significant (Fig. 3*A*,*D*,*I*). These histological findings are supported by ELISA results. $A\beta_{1-42}$ level increased significantly higher (1.6-fold higher) in the neocortex of the captopril-treated mice than in that of the control mice, whereas $A\beta_{1-40}$ level showed no significant increase in the neocortex of the captopril-treated mice (Fig. 3*E*,*F*). Consistent with a previous study (Kawarabayashi et al., 2001), the present study also showed that small "diffuse plaques" appear to be labeled preferentially by the anti-$A\beta_{1-42}$ antibody, whereas big "cored plaques" are labeled by the anti-$A\beta_{1-40}$ antibody (Fig. 3*A*). Captopril treatment decreased serum ACE activity by 40% and neocortex ACE activity by 26% in the 17-month-old captopril-treated Tg2576 mice compared with that in the control mice (Fig. 3*J*,*K*). The activity of brain ACE significantly and inversely correlated with enhanced thioflavin-S-positive plaque formation in the neocortex of the mice (Fig. 3*L*). These findings indicate that ACE inhibition promotes a greater degree of and earlier $A\beta_{1-42}$ deposition than $A\beta_{1-40}$ deposition, suggesting that a low ACE activity in the brain promotes AD development by enhancing $A\beta_{1-42}$ deposition.

To determine whether acute ACE inhibition has a direct effect on the levels of brain Aβs, we treated Tg2576 mice with captopril by one-shot oral gavage. The Tg2576 mice used for this experiment were 9 months of age, younger than those used for chronic treatment and supposed to have few Aβ deposits. The one-shot oral gavage of captopril (30 mg/kg of body weight in a volume of 150 μl) to Tg2576 mice resulted in a significant decrease in serum ACE activity (control, 248 ± 21 U/L; captopril-treated mice, 43 ± 2 U/L; $p < 0.01$, Mann–Whitney U test; $n = 6$ each group). The ACE activity in the neocortex of the captopril-treated mice was significantly lower than that of the control mice (control, 38 ± 4 mU/L; captopril-treated, 32 ± 5 mU/L; Mann–Whitney U test, $p < 0.05$; $n = 6$ each group). However, the acute ACE inhibition resulted in no significant increase in the level of $A\beta_{1-42}$ (control, 391 ± 99 pmol/g; captopril-treated mice, 619 ± 94 pmol/g; $p = 0.15$, Mann–Whitney U test; $n = 6$ each group) or $A\beta_{1-40}$ (control, 929 ± 164 pmol/g; captopril-treated mice, 1270 ± 156 pmol/g; $p = 0.20$, Mann–Whitney U test; $n = 6$ each group) in the Tg2576 mouse brain. These results suggest that ACE inhibition does not significantly alter brain Aβ degradation in the acute phase.

To exclude the possibility that captopril affects γ-secretase processing, thereby altering $A\beta_{42}/A\beta_{40}$ ratio, we treated fibroblasts stably expressing hAPP695 with captopril and quantified the secreted $A\beta_{1-40}$ and $A\beta_{1-42}$. No cellular ACE in this cell line was detected by Western blot analysis using several anti-ACE antibodies [MAB3500 and MAB3502 (Millipore); ACENabm-9B9 (RDI, Flanders, NJ); 2E2 (Serotec, Oxford, UK); 19501 (QED Bioscience, San Diego, CA); AF1513 (R & D Systems, Minneapolis, MN)] (Fig. 4*A*) (data not shown). No ACE activity was detected in this cell line either (Fig. 4*B*). We used a mouse kidney homogenate as a positive control. ACE and ACE activity in the kidney homogenate were clearly detected, and ACE activity was inhibited by captopril (Fig. 4*A*,*B*). The treatment with captopril did not alter $A\beta_{1-40}$ or $A\beta_{1-42}$ level or $A\beta_{42}/A\beta_{40}$ ratio in fibroblasts, indicating that captopril has no effect on γ-secretase activity in terms of the shift from $A\beta_{1-42}$ secretion to $A\beta_{1-40}$ secretion (Figs. 4*C*,*D*). These results suggest that the enhanced predominant $A\beta_{1-42}$ deposition in the captopril-treated Tg2576 mice is caused by the inhibition of ACE-mediated $A\beta_{1-42}$-to-$A\beta_{1-40}$-converting activity and $A\beta_{1-42}$ and $A\beta_{1-40}$ degradations, and not by altering γ-secretase processing.

Discussion

Here, we reported for the first time that ACE converts $A\beta_{1-42}$ to $A\beta_{1-40}$ and that a chronic inhibition of ACE enhances predominant $A\beta_{1-42}$ deposition *in vivo*. A high $A\beta_{1-42}$ level or a high $A\beta_{42}/A\beta_{40}$ ratio appears crucial in AD pathogenesis. Although their molecular mechanisms are not yet fully understood, $A\beta_{1-40}$ and $A\beta_{1-42}$ generations are supposed to be modulated by the shift of γ-cleavage (Weggen et al., 2001; De Strooper, 2003; Lleo et al., 2004). In addition to the γ-cleavage shift theory, $A\beta_{1-40}$ and $A\beta_{1-42}$ have recently been suggested to be generated from a longer form of Aβ species generated by ε-cleavage at every three residues in its carboxyl portion; however, the enzyme involved in carboxypeptidyl cleavage has not yet been identified (Qi-Takahara et al., 2005). Our present study showed a novel catabolism pathway for modulating $A\beta_{1-42}$ degradation; that is, ACE generates $A\beta_{1-40}$ from secreted $A\beta_{1-42}$ by carboxydipeptidyl cleavage in the mouse and human brains.

ACE is a zinc metallopeptidase and a dipeptidyl carboxypeptidase that cleaves 2 aa from the C terminus of Ang I and converts Ang I to the vasoactive and aldosterone-stimulating peptide Ang II (Corvol et al., 1995). ACE is a membrane-bound enzyme in endothelial cells and several types of epithelial and neuroepithelial cells. The active site of ACE is located in the extracellular space, and the unbound form of ACE circulating in biological fluids, such as plasma and CSF, and both types of ACE have enzymatic activity (Zubenko et al., 1985; Rigat et al., 1990; Sibony et al., 1993). These lines of evidence support our findings that ACE converts $A\beta_{1-42}$ to $A\beta_{1-40}$ and degrades Aβs under physiological conditions, thereby contributing to the prevention of Aβ deposition in the brain. In this study, ~10–20% of degraded $A\beta_{1-42}$ was converted to $A\beta_{1-40}$ in the presence of ACE.

Previous studies showed that the major cleavage site of $A\beta_{1-40}$ is between amino acid positions 7 and 8 (Hu et al., 2001; Oba et al., 2005). If the $A\beta_{1-40}$ generated from $A\beta_{1-42}$ was subsequently cleaved between amino positions 7 and 8 by ACE, then $A\beta_{8-40}$ could have been detected by MALDI-TOF-MS. However, no generation of $A\beta_{1-7}$, $A\beta_{8-40}$, or $A\beta_{8-42}$ in the reaction mixture of ACE and $A\beta_{1-42}$ was detected by MALDI-TOF-MS, indicating that no cleavage between amino positions 7 and 8 occurs in our system. What causes this discrepancy remains undetermined. It is possible that $A\beta_{1-42}$ and $A\beta_{1-40}$ have different conformations, which may allow ACE to access these species differently. Another explanation may be that the ACE used in this study contained the plasma membrane domain from the human kidney, and that

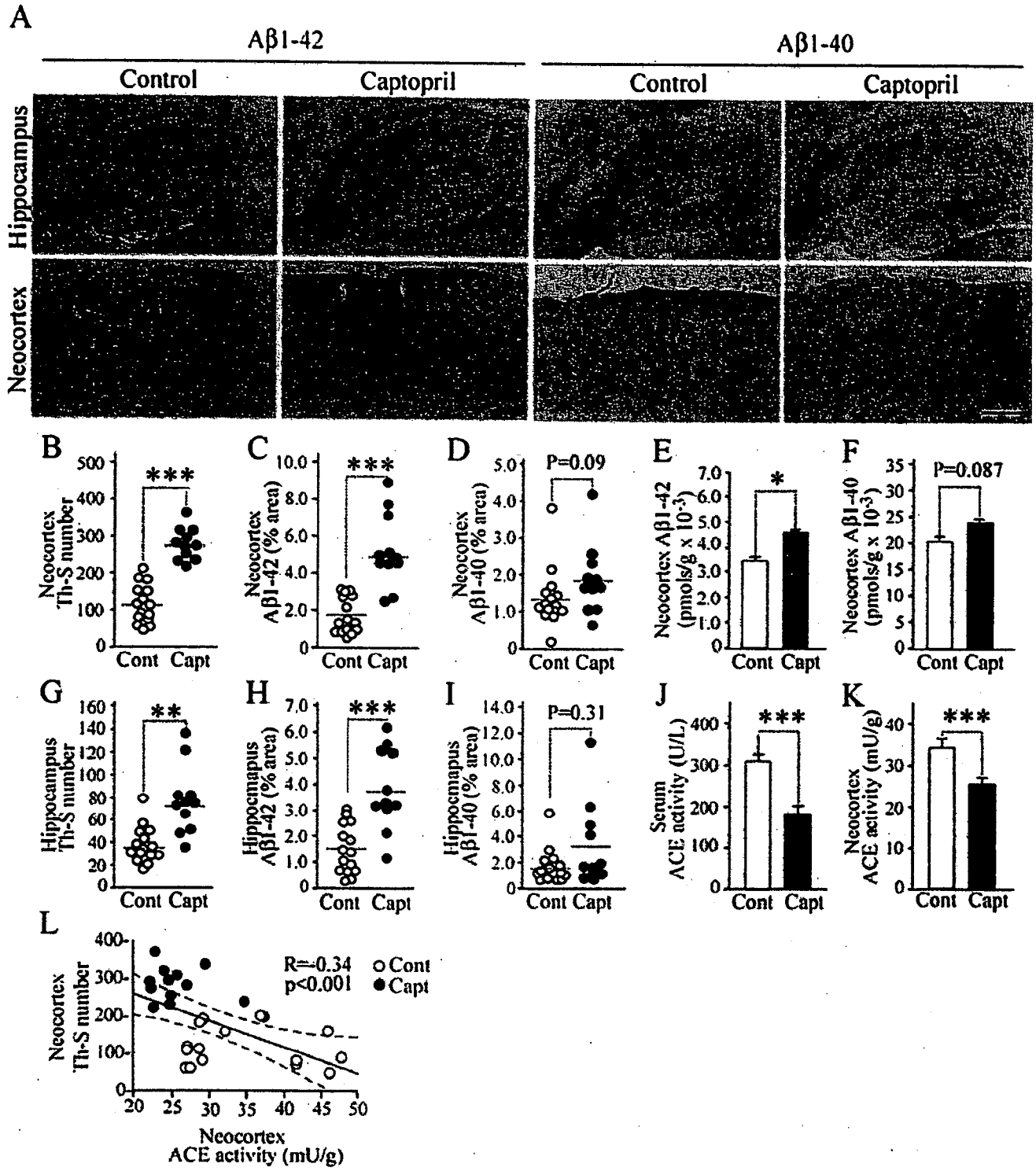

Figure 3. Long-term inhibition of ACE activity enhances $A\beta_{1-42}$ deposition in the 17-month-old hAPPsw transgenic mouse (Tg2576) brain. Tg2576 mice at 6 months of age were treated with captopril (30 mg/kg of body weight/d) and killed after 11 months of treatment. *A*, Sagittal brain sections of 17-month-old control diet-fed and captopril-supplemented diet-fed mice were stained with antibodies specific for $A\beta_{1-42}$ and $A\beta_{1-40}$ to detect human $A\beta$ deposition. Representative images of hippocampi and neocortices with or without treatment are shown. The left four panels are images immunostained by the anti-$A\beta_{1-42}$ antibody, and the right four panels are images of brain sections immunostained by the anti-$A\beta_{1-40}$ antibody. Scale bar, 500 μm. *B–I*, Determinations of the number of thioflavin-S-positive plaques (*B*, *G*) and immunopositive area demonstrated by anti-$A\beta_{1-42}$ antibody (*C*, *H*) and anti-$A\beta_{1-40}$ antibody (*D*, *I*) in brain neocortex (*B–D*) and hippocampus [*G–I*; $n = 15$ for control diet (Cont; open circles); $n = 11$ for captopril diet (Capt; filled circles)]. *E*, *F*, $A\beta_{1-42}$ (*E*) and $A\beta_{1-40}$ (*F*) levels determined by ELISA in brain neocortex of 17-month-old mice fed with control and captopril-supplemented diets. The ELISA data included both soluble and insoluble $A\beta$s. *J*, *K*, Serum (*J*) and neocortex (*K*) ACE activities in mice fed with control diet and captopril-supplemented diet. *L*, Significant inverse correlation between ACE activity and the number of thioflavin-S-positive plaques in neocortex. Data are the mean ± SEM; *p* was determined by the Mann–Whitney *U* test (*B–K*) and Spearman rank test (*L*). $^*p < 0.05$; $^{**}p < 0.01$; $^{***}p < 0.001$.

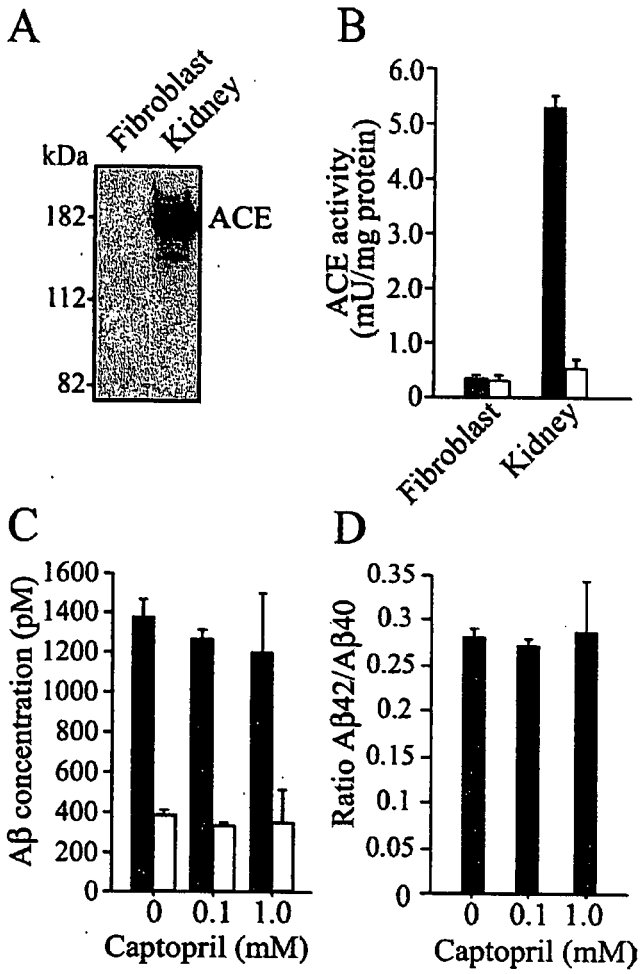

Figure 4. Effect of captopril on $A\beta_{1-42}/A\beta_{1-40}$ ratio in hAPP-expressing fibroblasts. *A*, Fibroblast homogenate and wild-type mouse kidney homogenate (40 μg of protein) were subjected to Western blot analysis using an anti-ACE polyclonal antibody. No cellular ACE in fibroblasts was detected, whereas ACE in the mouse kidney homogenate as a positive control was clearly detected. *B*, ACE activities in the fibroblast and kidney homogenates were determined. ACE activity in the fibroblast homogenate was very low, whereas that in kidney homogenate was detectable, which was clearly inhibited by captopril (1 μM) treatment (filled bars, no captopril; open bars, captopril). *C*, Fibroblasts stably expressing human APP695 were grown in DMEM containing 10% FBS. The cells were treated with or without captopril at 100% confluence after changing the culture medium. The $A\beta_{1-40}$ and $A\beta_{1-42}$ levels in the medium were determined by ELISA after 24 h. Filled bars, $A\beta_{1-40}$; open bars, $A\beta_{1-42}$. *D*, $A\beta_{42}/A\beta_{40}$ ratio was calculated. *C*, *D*, Note that captopril did not alter the levels of secreted Aβs (*C*) or $A\beta_{42}/A\beta_{40}$ ratio (*D*).

used in previous studies was the secreted form of ACE in human seminal plasma or Cos7-secreted conditioned media. Additional studies are required to clarify this. In this study, MALDI-TOF-MS demonstrated a peak corresponding to $A\beta_{1-40}$ in the reaction mixture of ACE and $A\beta_{1-42}$ but no peak corresponding to Aβ1–38. This suggests that ACE does not cleave the 2 C-terminal amino acids of $A\beta_{1-40}$.

In addition, one may question why $A\beta_{1-40}$ level increases if $A\beta_{1-40}$ can be digested further. It is possible that the most predominant substrate at the start of the reaction is $A\beta_{1-42}$ and that the degradation of $A\beta_{1-40}$ is negligible because the level of $A\beta_{1-40}$ generated from $A\beta_{1-42}$ is extremely low (Fig. 1*F*).

To understand the role of ACE *in vivo*, we induced a chronic ACE inhibition in Tg2576 mice and found that the ACE inhibition enhances Aβ deposition *in vivo*. However, it is important to determine whether acute and short-term treatment with captopril also increases brain soluble Aβ level. To exclude the effect of Aβ deposition, we used younger Tg2576 mice, whose brain shows almost no Aβ deposition (Kawarabayashi et al., 2001), in this experiment. An acute, one-shot oral administration of captopril to the young Tg2576 mice resulted in a significant decrease in serum and brain ACE activities; however, the level of brain $A\beta_{1-42}$ or $A\beta_{1-40}$ was not significantly affected. A recent *in vivo* study also shows that ACE inhibitors at doses similar to those used clinically do not increase the levels of brain Aβs (Eckman et al., 2006). Previous studies using purified human seminal plasma ACE and cultured cells showed that ACE degrades Aβs and ACE inhibition increases Aβ levels in APP- and ACE-transfected cells (Hu et al., 2001; Hemming and Selkoe, 2005; Oba et al., 2005). However, these findings seem to disagree with those of *in vivo* studies. One explanation may be that other Aβ-degrading enzymes, such as neprilysin, the insulin-degrading enzyme, and the endothelin-converting enzyme may compensate for the acute reduction in ACE activity *in vivo*. An important issue to be stressed is that even a high captopril dose induces only a slight decrease in brain ACE activity; however, long-term captopril treatment induces a marked and significant enhancement of Aβ deposition in the aged mouse brain. Thus, additional studies are required to determine the chronic effect of ACE inhibitors at clinical doses on AD pathology and development.

Numerous studies have shown that the I allele of ACE *D/I* polymorphism is associated with an increased risk of late-onset AD (Hu et al., 1999; Kehoe et al., 1999; Elkins et al., 2004; Lehmann et al., 2005) and that *I* polymorphism is associated with a decreased serum ACE level (Rigat et al., 1990). ACE activity in CSF from patients with a moderately severe senile dementia of the AD type has been shown to decrease to 41% of that in CSF from non-AD patients (Zubenko et al., 1985). Because ACE inhibitors are widely used in patients with hypertension, which is a risk factor for AD, it is important to determine the effects of ACE inhibitors on Aβ deposition *in vivo*. We have treated an AD mouse model (hAPPsw, Tg2576) (Hsiao et al., 1996) with captopril, a blood–brain barrier-penetrating ACE inhibitor, and found that, consistent with our *in vitro* findings, treatment with captopril enhances the depositions of $A\beta_{1-42}$ and $A\beta_{1-40}$, but more prominently that of $A\beta_{1-42}$ in mouse brains. This suggests that a certain amount of $A\beta_{1-40}$ is generated by ACE from secreted $A\beta_{1-42}$ and that treatment with ACE inhibitors may be a risk factor for AD. There have been very few clinical studies analyzing the effects of ACE inhibitors on AD development and cognitive decline in AD patients, and results to date are inconclusive (Birkenhager et al., 2004; Gard and Rusted, 2004; Ohrui et al., 2004; Khachaturian et al., 2006). Therefore, additional studies are required to determine the effects of ACE inhibitors both on Aβ deposition in the brain of patients during long-term medication with ACE inhibitors and on the cognitive ability of AD patients without hypertension. Together, the results of this study suggest that the upregulation of ACE activity may decrease $A\beta_{42}/A\beta_{40}$ ratio and the levels of Aβs and can be used as a strategy for developing novel therapeutic regimens for AD patients without hypertension.

References

Birkenhager WH, Forette F, Staessen JA (2004) Dementia and antihypertensive treatment. Curr Opin Nephrol Hypertens 13:225–230.

Borchelt DR, Thinakaran G, Eckman CB, Lee MK, Davenport F, Ratovitsky T, Prada CM, Kim G, Seekins S, Yager D, Slunt HH, Wang R, Seeger M, Levey AI, Gandy SE, Copeland NG, Jenkins NA, Price DL, Younkin SG, Sisodia SS (1996) Familial Alzheimer's disease-linked presenilin 1 variants elevate Aβ1–42/1–40 ratio in vitro and in vivo. Neuron 17:1005–1013.

Citron M, Westaway D, Xia W, Carlson G, Diehl T, Levesque G, Johnson-Wood K, Lee M, Seubert P, Davis A, Kholodenko D, Motter R, Sherrington R, Perry B, Yao H, Strome R, Lieberburg I, Rommens J, Kim S, Schenk D, et al. (1997) Mutant presenilins of Alzheimer's disease increase production of 42-residue amyloid β-protein in both transfected cells and transgenic mice. Nat Med 3:67–72.

Corvol P, Williams TA, Soubrier F (1995) Peptidyl dipeptidase A: angiotensin I-converting enzyme. Methods Enzymol 248:283–305.

De Strooper B (2003) Aph-1, Pen-2, and Nicastrin with presenilin generate an active γ-secretase complex. Neuron 38:9–12.

Duff K, Eckman C, Zehr C, Yu X, Prada CM, Perez-tur J, Hutton M, Buee L, Harigaya Y, Yager D, Morgan D, Gordon MN, Holcomb L, Refolo L, Zenk B, Hardy J, Younkin S (1996) Increased amyloid-β42(43) in brains of mice expressing mutant presenilin 1. Nature 383:710–713.

Eckman EA, Adams SK, Troendle FJ, Stodola BA, Kahn MA, Fauq AH, Xiao HD, Bernstein KE, Eckman CB (2006) Regulation of steady-state β-amyloid levels in the brain by neprilysin and endothelin-converting enzyme but not angiotensin-converting enzyme. J Biol Chem 281:30471–30478.

Elkins JS, Douglas VC, Johnston SC (2004) Alzheimer disease risk and genetic variation in ACE: a meta-analysis. Neurology 62:363–368.

Gard PR, Rusted JM (2004) Angiotensin and Alzheimer's disease: therapeutic prospects. Expert Rev Neurother 4:87–96.

Hayakari M, Satoh K, Izumi H, Kudoh T, Asano J, Yamazaki T, Tsuchida S (2003) Kinetic-controlled hydrolysis of Leu-Val-Val-hemorphin-7 catalyzed by angiotensin-converting enzyme from rat brain. Peptides 24:1075–1082.

Hemming ML, Selkoe DJ (2005) Amyloid β-protein is degraded by cellular angiotensin-converting enzyme (ACE) and elevated by an ACE inhibitor. J Biol Chem 280:37644–37650.

Hsiao K, Chapman P, Nilsen S, Eckman C, Harigaya Y, Younkin S, Yang F, Cole G (1996) Correlative memory deficits, Aβ elevation, and amyloid plaques in transgenic mice. Science 274:99–102.

Hu J, Miyatake F, Aizu Y, Nakagawa H, Nakamura S, Tamaoka A, Takahash R, Urakami K, Shoji M (1999) Angiotensin-converting enzyme genotype is associated with Alzheimer disease in the Japanese population. Neurosci Lett 277:65–67.

Hu J, Igarashi A, Kamata M, Nakagawa H (2001) Angiotensin-converting enzyme degrades Alzheimer amyloid β-peptide (Aβ); retards Aβ aggregation, deposition, fibril formation; and inhibits cytotoxicity. J Biol Chem 276:47863–47868.

in 't Veld BA, Ruitenberg A, Hofman A, Launer LJ, van Duijn CM, Stijnen T, Breteler MM, Stricker BH (2001) Nonsteroidal antiinflammatory drugs and the risk of Alzheimer's disease. N Engl J Med 345:1515–1521.

Iwatsubo T, Odaka A, Suzuki N, Mizusawa H, Nukina N, Ihara Y (1994) Visualization of Aβ42(43) and Aβ40 in senile plaques with end-specific Aβ monoclonals: evidence that an initially deposited species is Aβ42(43). Neuron 13:45–53.

Johnson-Wood K, Lee M, Motter R, Hu K, Gordon G, Barbour R, Khan K, Gordon M, Tan H, Games D, Lieberburg I, Schenk D, Seubert P, McConlogue L (1997) Amyloid precursor protein processing and Aβ42 deposition in a transgenic mouse model of Alzheimer disease. Proc Natl Acad Sci USA 94:1550–1555.

Kawarabayashi T, Younkin LH, Saido TC, Shoji M, Ashe KH, Younkin SG (2001) Age-dependent changes in brain, CSF, and plasma amyloid β-protein in the Tg2576 transgenic mouse model of Alzheimer's disease. J Neurosci 21:372–381.

Kehoe PG, Russ C, McIlory S, Williams H, Holmans P, Holmes C, Liolitsa D, Vahidassr D, Powell J, McGleenon B, Liddell M, Plomin R, Dynan K, Williams N, Neal J, Cairns NJ, Wilcock G, Passmore P, Lovestone S, Williams J, et al. (1999) Variation in DCP1, encoding ACE, is associated with susceptibility to Alzheimer disease. Nat Genet 21:71–72.

Khachaturian AS, Zandi PP, Lyketsos CG, Hayden KM, Skoog I, Norton MC, Tschanz JT, Mayer LS, Welsh-Bohmer KA, Breitner JC (2006) Antihypertensive medication use and incident Alzheimer disease: the Cache County Study. Arch Neurol 63:686–692.

Kirkitadze MD, Bitan G, Teplow DB (2002) Paradigm shifts in Alzheimer's disease and other neurodegenerative disorders: the emerging role of oligomeric assemblies. J Neurosci Res 69:567–577.

Lehmann DJ, Cortina-Borja M, Warden DR, Smith AD, Sleegers K, Prince JA, van Duijn CM, Kehoe PG (2005) Large meta-analysis establishes the ACE insertion-deletion polymorphism as a marker of Alzheimer's disease. Am J Epidemiol 162:305–317.

Levine III H (1995) Soluble multimeric Alzheimer β(1–40) pre-amyloid complexes in dilute solution. Neurobiol Aging 16:755–764.

Levine III H (1999) Quantification of β-sheet amyloid fibril structures with thioflavin T. Methods Enzymol 309:274–284.

Lleo A, Berezovska O, Herl L, Raju S, Deng A, Bacskai BJ, Frosch MP, Irizarry M, Hyman BT (2004) Nonsteroidal anti-inflammatory drugs lower Aβ42 and change presenilin 1 conformation. Nat Med 10:1065–1066.

McGowan E, Pickford F, Kim J, Onstead L, Eriksen J, Yu C, Skipper L, Murphy MP, Beard J, Das P, Jansen K, Delucia M, Lin WL, Dolios G, Wang R, Eckman CB, Dickson DW, Hutton M, Hardy J, Golde T (2005) Aβ42 is essential for parenchymal and vascular amyloid deposition in mice. Neuron 47:191–199.

Morishima-Kawashima M, Oshima N, Ogata H, Yamaguchi H, Yoshimura M, Sugihara S, Ihara Y (2000) Effect of apolipoprotein E allele epsilon4 on the initial phase of amyloid β-protein accumulation in the human brain. Am J Pathol 157:2093–2099.

Oba R, Igarashi A, Kamata M, Nagata K, Takano S, Nakagawa H (2005) The N-terminal active centre of human angiotensin-converting enzyme degrades Alzheimer amyloid β-peptide. Eur J Neurosci 21:733–740.

Ohrui T, Tomita N, Sato-Nakagawa T, Matsui T, Maruyama M, Niwa K, Arai H, Sasaki H (2004) Effects of brain-penetrating ACE inhibitors on Alzheimer disease progression. Neurology 63:1324–1325.

Plant LD, Boyle JP, Smith IF, Peers C, Pearson HA (2003) The production of amyloid β-peptide is a critical requirement for the viability of central neurons. J Neurosci 23:5531–5535.

Qi-Takahara Y, Morishima-Kawashima M, Tanimura Y, Dolios G, Hirotani N, Horikoshi Y, Kametani F, Maeda M, Saido TC, Wang R, Ihara Y (2005) Longer forms of amyloid β-protein: implications for the mechanism of intramembrane cleavage by γ-secretase. J Neurosci 25:436–445.

Rigat B, Hubert C, Alhenc-Gelas F, Cambien F, Corvol P, Soubrier F (1990) An insertion/deletion polymorphism in the angiotensin I-converting enzyme gene accounting for half the variance of serum enzyme levels. J Clin Invest 86:1343–1346.

Scheuner D, Eckman C, Jensen M, Song X, Citron M, Suzuki N, Bird TD, Hardy J, Hutton M, Kukull W, Larson E, Levy-Lahad E, Viitanen M, Peskind E, Poorkaj P, Schellenberg G, Tanzi R, Wasco W, Lannfelt L, Selkoe D, et al. (1996) Secreted amyloid β-protein similar to that in the senile plaques of Alzheimer's disease is increased in vivo by the presenilin 1 and 2 and APP mutations linked to familial Alzheimer's disease. Nat Med 2:864–870.

Selkoe DJ (2004) Cell biology of protein misfolding: the examples of Alzheimer's and Parkinson's diseases. Nat Cell Biol 6:1054–1061.

Shiraishi H, Sai X, Wang HQ, Maeda Y, Kurono Y, Nishimura M, Yanagisawa K, Komano H (2004) PEN-2 enhances γ-cleavage after presenilin heterodimer formation. J Neurochem 90:1402–1413.

Sibony M, Gasc JM, Soubrier F, Alhenc-Gelas F, Corvol P (1993) Gene expression and tissue localization of the two isoforms of angiotensin I converting enzyme. Hypertension 21:827–835.

Walsh DM, Klyubin I, Fadeeva JV, Cullen WK, Anwyl R, Wolfe MS, Rowan MJ, Selkoe DJ (2002) Naturally secreted oligomers of amyloid β-protein potently inhibit hippocampal long-term potentiation in vivo. Nature 416:535–539.

Weggen S, Eriksen JL, Das P, Sagi SA, Wang R, Pietrzik CU, Findlay KA, Smith TE, Murphy MP, Bulter T, Kang DE, Marquez-Sterling N, Golde TE, Koo EH (2001) A subset of NSAIDs lower amyloidogenic Aβ42 independently of cyclooxygenase activity. Nature 414:212–216.

Wyss-Coray T, Lin C, Yan F, Yu GQ, Rohde M, McConlogue L, Masliah E, Mucke L (2001) TGF-beta1 promotes microglial amyloid-β clearance and reduces plaque burden in transgenic mice. Nat Med 7:612–618.

Zou K, Gong JS, Yanagisawa K, Michikawa M (2002) A novel function of monomeric amyloid β-protein serving as an antioxidant molecule against metal-induced oxidative damage. J Neurosci 22:4833–4841.

Zou K, Kim D, Kakio A, Byun K, Gong JS, Kim J, Kim M, Sawamura N, Nishimoto S, Matsuzaki K, Lee B, Yanagisawa K, Michikawa M (2003) Amyloid β-protein (Aβ)1–40 protects neurons from damage induced by Aβ1–42 in culture and in rat brain. J Neurochem 87:609–619.

Zubenko GS, Volicer L, Direnfeld LK, Freeman M, Langlais PJ, Nixon RA (1985) Cerebrospinal fluid levels of angiotensin-converting enzyme in Alzheimer's disease, Parkinson's disease and progressive supranuclear palsy. Brain Res 328:215–221.

THE JOURNAL OF BIOLOGICAL CHEMISTRY VOL. 282, NO. 4, pp. 2646–2655, January 26, 2007

A Ganglioside-induced Toxic Soluble Aβ Assembly

*ITS ENHANCED FORMATION FROM Aβ BEARING THE ARCTIC MUTATION**

Received for publication, June 29, 2006, and in revised form, November 27, 2006 Published, JBC Papers in Press, November 29, 2006, DOI 10.1074/jbc.M606202200

Naoki Yamamoto[‡§], Etsuro Matsubara[‡], Sumihiro Maeda[¶], Hirohisa Minagawa[‡], Akihiko Takashima[¶], Wakako Maruyama[‖], Makoto Michikawa[‡], and Katsuhiko Yanagisawa[‡1]

From the Departments of [‡]Alzheimer's Disease Research and [‖]Geriatric Medicine, National Institute for Longevity Sciences, National Center for Geriatrics and Gerontology, Obu 474-8522, Japan, the [§]Japan Society for the Promotion of Sciences, Tokyo 102-8472, Japan, and the [¶]Laboratory for Alzheimer's Disease, RIKEN Brain Science Institute, Wako 351-0198, Japan

The mechanism underlying plaque-independent neuronal death in Alzheimer disease (AD), which is probably responsible for early cognitive decline in AD patients, remains unclarified. Here, we show that a toxic soluble Aβ assembly (TAβ) is formed in the presence of liposomes containing GM1 ganglioside more rapidly and to a greater extent from a hereditary variant-type ("Arctic") Aβ than from wild-type Aβ. TAβ is also formed from soluble Aβ through incubation with natural neuronal membranes prepared from aged mouse brains in a GM1 ganglioside-dependent manner. An oligomer-specific antibody (anti-Oligo) significantly suppresses TAβ toxicity. Biophysical and structural analyses by atomic force microscopy and size exclusion chromatography revealed that TAβ is spherical with diameters of 10–20 nm and molecular masses of 200–300 kDa. TAβ induces neuronal death, which is abrogated by the small interfering RNA-mediated knockdown of nerve growth factor receptors, including TrkA and p75 neurotrophin receptor. Our results suggest that soluble Aβ assemblies, such as TAβ, can cause plaque-independent neuronal death that favorably occurs in nerve growth factor-dependent neurons in the cholinergic basal forebrain in AD.

The poor correlation between amyloid load in the brain and the degree of neurological deficits in patients with Alzheimer disease (AD)[2] (1) or animal models of AD (2, 3) argues against amyloid fibrils being the primary toxic Aβ species. Recently, soluble Aβ assemblies, also referred to as Aβ oligomers (4), protofibrils (5, 6), or Aβ-derived diffusible ligands (7), have attracted attention because of their potency to impair neuronal function or induce neuritic degeneration (7–13). Several possibilities have been proposed in regard to the toxicities of soluble Aβ assemblies (*e.g.* the binding of assemblies to target molecules on neuronal membranes (7, 14) and the ubiquitous disruption of the plasma membrane in association with the perturbation of ionic homeostasis (15)). It is also noteworthy that neurotoxicities induced by soluble Aβ assemblies are mediated, at least in part, by the activation of signal transduction pathways, including those involving Src family kinases, extracellular signal-regulated kinase, or sphingomyelinases (7, 11, 16, 17). Notably, the level of soluble Aβ assemblies increases in the brain and cerebrospinal fluid of AD patients (18, 19, 20, 21, 22), and oligomer-specific immunoreactivity is readily observed in the AD brain (23). Furthermore, the inhibition of long term potentiation and the impairment of cognitive function *in vivo* can be induced by natural Aβ oligomers (9, 24) or a specific Aβ assembly called Aβ*56, which has recently been isolated from *Tg2576* mice (expressing a human amyloid precursor protein variant-linked familial AD) (25). Additionally, recent studies using AD mouse models revealed that soluble Aβ assemblies may play a role in the induction of tau pathology (26) and that the genetic deletion of β-secretase, which is responsible for Aβ production, rescues temporal memory deficit in conjunction with the suppression of the increase in the levels of cerebral Aβ-derived diffusible ligands (27). These lines of evidence indicate the pathological relevance of these soluble Aβ assemblies in AD development. However, it remains to be elucidated how these assemblies are formed *in vivo*.

Several mutations within the Aβ sequence have been reported to be responsible for the development of familial AD and hereditary cerebral amyloid angiopathy (28–32). Among these mutations, the Arctic mutation, unlike other mutations, accelerates the development of clinical and neuropathological features indistinguishable from those of sporadic AD, although it does not increase Aβ42 level or Aβ42/Aβ40 ratio (30). The pathological features induced by the Arctic mutation, including predominant Aβ deposition in the brain parenchyma, have also been confirmed in transgenic mice (33). Notably, Aβ bearing the Arctic mutation shows a propensity to form neurotoxic nonamyloid assemblies, including protofibrils, amyloid pores, and small nonfibrillar assemblies (13, 30, 34). Thus, researchers have focused on the Arctic mutation in terms of the mechanisms underlying the formation of soluble and insoluble Aβ assemblies.

In regard to the assembly of wild-type and hereditary variant-type Aβs, we have recently observed that Arctic-type Aβ, unlike other hereditary variant-type Aβs (*i.e.* Dutch-type, Italian-type,

* This study was supported by Grant-in-aid for Scientific Research on Priority Areas 1700220004, Research on Pathomechanisms of Brain Disorders, from the Ministry of Education, Culture, Sports, Science and Technology of Japan. The costs of publication of this article were defrayed in part by the payment of page charges. This article must therefore be hereby marked "*advertisement*" in accordance with 18 U.S.C. Section 1734 solely to indicate this fact.

[1] To whom correspondence should be addressed: Dept. of Alzheimer's Disease Research, National Institute for Longevity Sciences, National Center for Geriatrics and Gerontology, 36-3 Gengo, Morioka, Obu 474-8522, Japan. Tel.: 81-562-44-5651 (ext. 5002); Fax: 81-562-44-6594; E-mail: katuhiko@nils.go.jp.

[2] The abbreviations used are: AD, Alzheimer disease; TAβ, toxic soluble Aβ assembly; NGF, nerve growth factor; LDH, lactate dehydrogenase; siRNA, small interfering RNA; AFM, atomic force microscopy; GM1, Galβ1,3GalNAcβ1,4(Neu5Ac-α2,3)Galβ1,4Glcβ1,1-ceramide; ThT, thioflavin-T; NTR, neurotrophin receptor.

and Flemish-type Aβs), preferably assembles in the presence of GM1 ganglioside, as does wild-type Aβ (35, 36). We also reported that GM1 ganglioside level increases in synaptosomes prepared from aged, human apolipoprotein E4 knock-in mice (37). Thus, it is possible that an alteration in the expression or distribution of GM1 ganglioside is the background to the assembly and deposition of Aβ in the brain parenchyma. This possibility has been supported by findings of recent studies as follows: 1) GM1 ganglioside level increases in membrane microdomains isolated from the frontal cortex but not from the temporal cortex, reflecting earlier and later stages of AD pathology, respectively (38), and 2) GM1 ganglioside level also increases in amyloid-positive nerve terminals obtained from the AD cortex (39).

In this study, we aimed to characterize the toxicity of assemblies formed from Arctic-type Aβ in the presence of GM1 ganglioside. We found that a toxic soluble Aβ assembly (TAβ) is formed more rapidly and to a greater extent from Arctic-type Aβ in the presence of GM1 ganglioside than from wild-type Aβ. Furthermore, our results suggest that TAβ induces nerve growth factor (NGF) receptor-mediated neuronal death. Thus, we propose that soluble Aβ assemblies, such as TAβ, are responsible for plaque-independent neuronal death that favorably occurs in NGF-dependent neurons in AD.

MATERIALS AND METHODS

Preparation of Seed-free Aβ Solutions and Liposomes—Synthetic wild-type Aβ (Aβ40) and Arctic-type Aβ (Aβ40) (Peptide Institute, Osaka, Japan) were dissolved in 0.02% ammonia solution at 500 μM. To obtain seed-free Aβ solutions, the prepared solutions were centrifuged at 540,000 × *g* for 3 h using an Optima TL ultracentrifuge (Beckman) to remove undissolved peptides that can act as preexisting seeds. The supernatant was collected and stored in aliquots at −80 °C until use. Immediately before use, the aliquots were thawed and diluted with Tris-buffered saline (150 mM NaCl and 10 mM Tris-HCl, pH 7.4). To prepare liposomes, cholesterol (Sigma), sphingomyelin (Sigma), and GM1 ganglioside (Matreya LLC) were dissolved in chloroform/methanol at a molar lipid ratio of 50:50:0, 45:45:10, 42.5:42.5:15, or 40:40:20. The mixtures were stored at −80 °C until use. Immediately before use, the lipids were resuspended in Tris-buffered saline at a ganglioside concentration of 2.5 mM, and the suspension was subjected to freezing and thawing and sonication.

Cell Culture—Cerebral cortical neurons were prepared from embryonic day 17 Sprague-Dawley rats and cultured in a serum-free medium consisting of Dulbecco's modified Eagle's medium nutrient mixture and N2 supplement. Rat pheochromocytoma PC12 (PC12) cells were cultured in Dulbecco's modified Eagle's medium (Invitrogen) supplemented with 10% heat-inactivated horse serum (Invitrogen) and 5% fetal bovine serum (Invitrogen). For their differentiation, PC12 cells were plated on 2-cm^2 poly-L-lysine-coated (10 mg/ml) dishes at a density of 20,000 cells/cm^2 and cultured for 6 days in Dulbecco's modified Eagle's medium supplemented with 100 ng/ml NGF (PC12N) (Alomone Laboratories, Jerusalem, Israel). Human neuroblastoma SH-SY5Y (SY5Y) cells were cultured in Dulbecco's modified Eagle's medium/Ham's F-12 medium supplemented with 10% fetal bovine serum. All of the cells were cultured in humidified 5% CO_2 at 37 °C.

Aβ Incubation in the Presence of GM1 Ganglioside—A seed-free Aβ solution was incubated at 37 °C and 50 μM, unless otherwise indicated, in the presence or absence of GM1 ganglioside-containing liposomes, as previously reported (40). The concentration of GM1 ganglioside in the incubation mixtures was 500 μM, and the molar ratio of GM1 ganglioside in the liposomes varied, as indicated in each figure.

ThT Assay—Aβ solutions were incubated in the presence of liposomes at 50 μM and 37 °C for various durations. The ThT fluorescence intensity of the incubation mixtures was determined using a spectrofluorophotometer (RF-5300PC) (Shimadzu Co., Kyoto, Japan). The optimum fluorescence intensity of amyloid fibrils was measured at excitation and emission wavelengths of 446 and 490 nm, respectively, with the reaction mixture (1.0 ml) containing 5 μM ThT and 50 mM glycine-NaOH at pH 8.5. The fluorescence intensity was measured immediately after preparing the mixture.

LDH Release Assay—The LDH assay was performed on medium using an LDH assay toxicity kit (Promega, Madison, WI). The degree of LDH release in each sample was assessed by measuring absorbance at 490 nm using an Emax precision microplate reader (Molecular Devices Corp., Sunnyvale, CA). Background absorbances, as assessed using cell-free wells, were subtracted from the absorbances of each test sample. Absorbances measured from three wells were averaged, and the percentage degree of LDH release was calculated by dividing the absorbance measured from each test sample following treatment with 1% Triton X-100 to induce the release of intracellular LDH according to instructions provided by the manufacturer.

Electron and Atomic Force Microscopies—For electron microscopy, the samples were diluted with distilled water and spread onto carbon-coated grids. The grids were negatively stained with 2% uranyl acetate and examined under a JEM-2000EX transmission electron microscope (Tokyo, Japan) with an acceleration voltage of 100 kV. Atomic force microscopy (AFM) assessment was performed as described elsewhere (41). Briefly, the samples were dropped onto a freshly cleaved mica. After leaving them to stand for 3 min and then washing with water, the samples were assessed in a solution using a Nanoscope IIIa (Digital Instruments, Santa Barbara, CA) set in the tapping mode (42). OMCL-TR400PSA (Olympus, Japan) was used as a cantilever. The resonant frequency was ~9 kHz.

Size Exclusion Chromatography—The molecular mass of TAβ was determined using a Superose 12 size exclusion column (1 × 30 cm; GE Healthcare) equilibrated with phosphate-buffered saline (pH 7.4) at a flow rate of 0.5 ml/min. Thirty-five fractions were collected and analyzed by dot blotting using anti-Oligo.

Preparation of Synaptosomes—Synaptosomes were prepared as previously described (43). A hippocampus or a whole brain minus the hippocampus was homogenized in 0.32 M sucrose buffer containing 0.25 mM EDTA. The homogenate was centrifuged at 580 × *g* for 8 min. The supernatant was centrifuged at 145,000 × *g* for 20 min. The resulting pellet was suspended in 0.32 M sucrose buffer without EDTA and layered over Ficoll in sucrose buffer. Following centrifugation at 87,000 × *g* for 30

min, the synaptosome-rich interface was removed and recentrifuged to remove any remaining Ficoll.

RNA Interference—Stealth™ small interfering RNA (siRNA) duplex oligoribonucleotides against PC12 cell TrkA (GenBank™ number NM_021589) and the p75 neurotrophin receptor ($p75^{NTR}$) (GenBank™ number NM_012610) were synthesized by Invitrogen. The siRNA sequences used were as follows: rTrkA-siRNA (position 1370) sense (5′-GCCCUCCUCCUAGUGCUCAACAAAU-3′) and antisense (5′-AUUUGUUGAGCACUAGGAGGAGGGC-3′); rTrkA-siRNA-control sense (5′-GCCCUCCGAUCUCGUCAACAUCAAU-3′) and antisense (5′-AUUGAUGUUGACGAGAUCGGAGGGC-3′); rp75-siRNA (position 1212) sense (5′-CAGCCUGAACAUAUAGACUCCUUUA-3′) and antisense (5′-UAAAGGAGUCUUAUAUGUUCAGGCUG-3′); rp75-siRNA-control sense (5′-CAGGUAAACAUAUAGUCCCUCCUUA-3′) and antisense (5′-UAAGGAGGGACUAUAUGUUUACCUG-3′). The control siRNA had a random sequence. siRNA oligonucleotides were transfected into PC12 cells using Lipofectamine 2000 (Invitrogen) according to the manufacturer's protocol.

RESULTS

Toxicity of Aβ Assembly Formed from Arctic-type Aβ—We treated primary neurons with seed-free wild- or Arctic-type Aβ, which had been preincubated for 2 h in the absence or presence of GM1 ganglioside (10 or 20% molar ratio in the lipids composing liposomes). Unexpectedly, extensive neuronal death was observed in the culture treated with Arctic-type Aβ, which had been preincubated for 2 h in the presence of GM1 ganglioside at a 10% molar ratio in liposomes (Fig. 1*A*). The extent of neuronal death under this condition was greater than that under any other conditions examined in this study (Fig. 1, *A* and *B*).

To quantitatively characterize the toxic Aβ assembly, we examined its toxicity against NGF-treated PC12 cells (PC12N cells). We found that PC12N cells are also sensitive to the toxic Aβ assembly formed from Arctic-type Aβ (Fig. 1*C*). We performed an LDH release assay of cultures of PC12N cells under various conditions. The level of LDH released from the PC12N cells, which were treated with the toxic Aβ assembly, increased depending on Aβ dose (Fig. 1*D*), GM1 ganglioside dose (Fig. 1*E*), and the duration of the exposure of the cells to the toxic Aβ assembly (Fig. 1*F*). In regard to the time course of Aβ preincubation with GM1 ganglioside, the level of released LDH increased with peak value at 2 h and then decreased in conjunction with an increase in the ThT fluorescence intensity of the incubation mixtures (Fig. 1*G*).

The Toxic Aβ Assembly Is Soluble—Importantly, the toxicity of the Aβ incubated in the presence of GM1 ganglioside was observed exclusively in the supernatant obtained by ultracentrifuging the incubation mixture (Fig. 2*A*), suggesting that the toxic Aβ assembly is soluble. To examine the possibility that a TAβ is formed in the presence GM1 ganglioside, we performed dot blotting using an oligomer-specific antibody (anti-Oligo) (23). TAβ in the incubation mixtures was readily recognized by anti-Oligo (Fig. 2*B*). The specificity of TAβ recognition by anti-Oligo was confirmed by the finding that TAβ toxicity was significantly neutralized by coincubating the mixtures with anti-Oligo in the cultures of PC12N cells and primary neurons (Fig. 2*C*). However, coincubation with a monoclonal antibody (4396C), which inhibits Aβ fibrillogenesis through binding to GM1 ganglioside-bound Aβ as a seed (40), failed to inhibit the induction of TAβ toxicity (Fig. 2*D*).

TAβ Formation from Wild-type Aβ—We then examined whether TAβ is also formed from wild-type Aβ (Aβ40). We first investigated how TAβ is formed from wild-type Aβ in the presence of liposomes containing GM1 ganglioside. Interestingly, TAβ is favorably formed from wild-type Aβ in the presence of GM1 ganglioside at a 15% molar ratio in liposomes (Fig. 3*A*). TAβ toxicity was not significant in the nanomolar range of Aβ (Fig. 3*B*).

Biophysical and Structural Features of TAβ—To determine the biophysical and structural features of TAβ, we performed SDS-PAGE of the incubation mixtures containing TAβ. However, no high molecular weight bands corresponding to possible Aβ assemblies were detected. Bands were observed only after cross-linking pretreatment with glutaraldehyde (Fig. 4*A*), consistent with previous findings showing that soluble Aβ assemblies are probably degraded by denaturing gel electrophoresis (6) unless they are cross-linked (44, 45). A morphological analysis of TAβ by electron microscopy failed to detect any definite structure under conditions in which protofibrils, which had been prepared as previously reported (30), were readily detectable (Fig. 4*B*). In contrast, spherical particles with diameters of 10–20 nm, along with rod-shaped structures, were observed by AFM in the supernatant obtained by ultracentrifuging the incubation mixtures containing TAβ (Fig. 4*C*). We then determined the molecular mass of TAβ by size exclusion chromatography, which was followed by dot blotting using anti-Oligo. The immunoreactivity was recovered as a single peak with relative molecular masses of 200–300 kDa (Fig. 4*D*). The recovery of TAβ immunoreactivity in the same fraction was also observed in the incubation mixture containing wild-type Aβ (Aβ40) and GM1 ganglioside at a 15% molar ratio in liposomes (Fig. 4*D*). Furthermore, the collected peak showed a significant toxicity against PC12N cells (Fig. 4*E*).

TAβ Formation in the Presence of Natural Neuronal Membranes—Next, we tested whether TAβ can be formed in the presence of natural neuronal membranes. We incubated Arctic-type Aβ in the presence of synaptosomes prepared from brains of mice from three different age groups. The degree of TAβ formation was significantly higher in the incubation mixture containing synaptosomes prepared from the hippocampus of aged (2-year-old) mouse brains than in any other incubation mixtures, including those containing synaptosomes from the hippocampus or the whole brain minus the hippocampus from younger (1-month-old and 1-year-old) mouse brains (Fig. 5*A*). To determine the possibility that an alteration in the lipid composition of neuronal membranes, particularly GM1 ganglioside, underlies the acceleration of TAβ formation, we determined the levels of GM1 ganglioside, cholesterol, and phospholipids in synaptosomes prepared from hippocampi of young (1-month-old) and aged (2-year-old) mouse brains. Notably, the GM1 ganglioside level significantly increased, whereas cholesterol level significantly decreased with age (Fig. 5*B*).

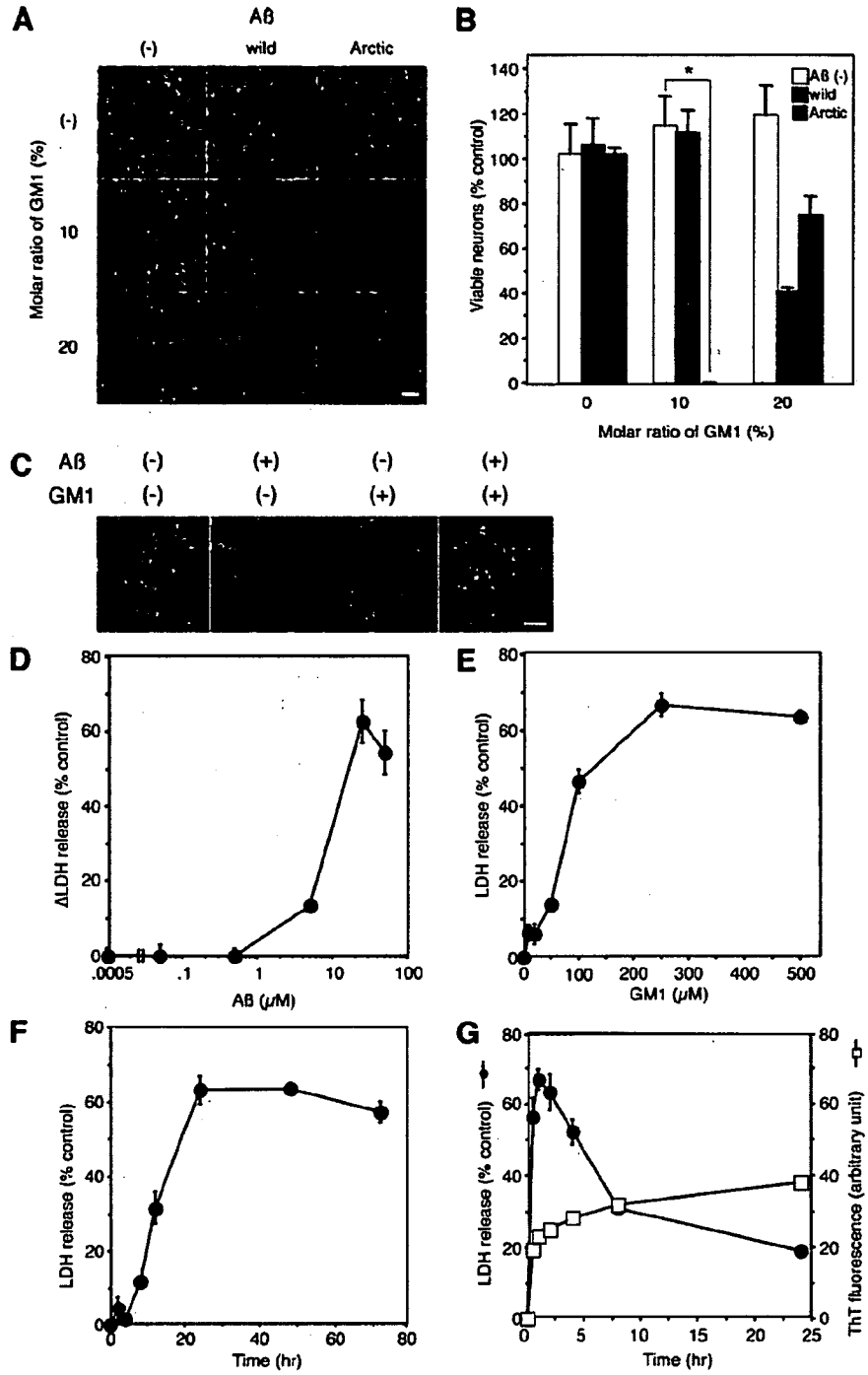

FIGURE 1. **Toxicity of Aβ assembly formed in the presence of GM1 ganglioside against primary neurons and PC12N cells.** *A*, primary cortical neurons cultured for 48 h in serum-free N2-supplemented medium were treated at 37 °C for 48 h with incubation mixtures containing seed-free wild-type Aβ (Aβ40) or Arctic-type Aβ (Aβ40) at a final concentration of 25 μM, which had been preincubated at 50 μM and 37 °C for 2 h in the absence or presence of GM1 ganglioside-containing liposomes. The GM1 ganglioside concentration in the incubation mixtures was 500 μM; the molar ratio of GM1 ganglioside in liposomes varied as indicated. Neurons were stained with calcein AM (Invitrogen)/ethidium homodimer, showing green staining for viable cells and *red* staining for dead cells. *Bar*, 50 μm. *B*, the number of viable neurons in the culture shown in *A* was determined. Each *column* indicates the average of three percentages ± S.D. relative to that of control cultures in which neither Aβ nor GM1 ganglioside was added. *, $p < 0.0001$ (one-way analysis of variance combined with Scheffe's test). *C*, representative images of NGF-treated PC12 (PC12N) cells treated at 37 °C for 48 h with incubation mixtures containing Arctic-type Aβ (Aβ40) at a final concentration of 25 μM, which had been preincubated at 50 μM and 37 °C for 2 h in the absence or presence of GM1 ganglioside-containing liposomes. The GM1 ganglioside concentration in the incubation mixtures was 500 μM, and the molar ratio of GM1 ganglioside in liposomes was 10%. *Bar*, 50 μm. *D* and *E*, dose-response curves for the level of LDH released from cells treated with incubation mixtures containing Aβ, which had been preincubated as described in *C*. The concentrations of Aβ and GM1 ganglioside varied as indicated. The LDH value indicates the percentage level of LDH released following treatment with incubation mixtures relative to the level of LDH released following treatment with Triton X-100. *D*, the points indicate LDH levels in the incubation mixtures containing GM1 ganglioside minus those lacking GM1 gangliosides, which were negligible below 25 μM Aβ. *F* and *G*, time course curves for level of LDH released from the cells treated with incubation mixtures containing Aβ, which had been preincubated as described in *A*. The durations of cell treatment (*F*) and Aβ preincubation in the presence of GM1 ganglioside (*G*) varied as indicated. ThT fluorescence intensities in the incubation mixtures are also shown in *G*. *D–G*, each point indicates the average of four values ± S.D.

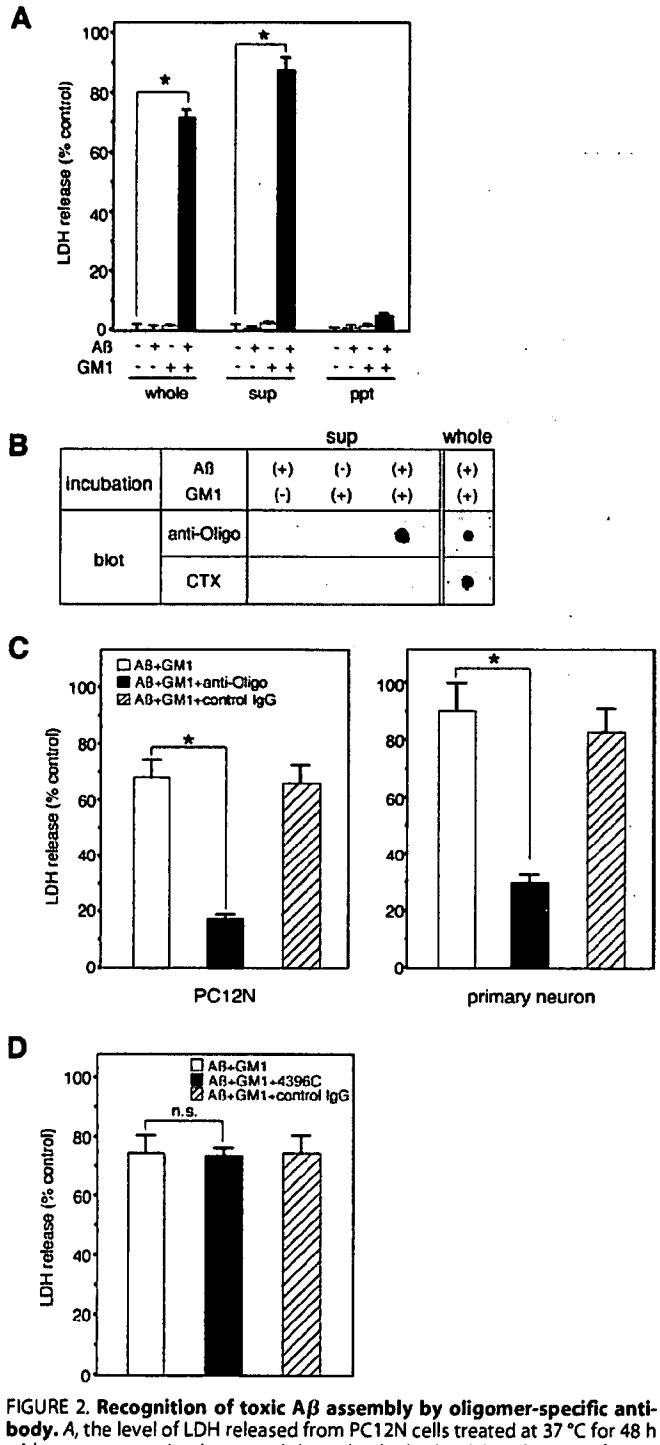

FIGURE 2. **Recognition of toxic Aβ assembly by oligomer-specific antibody.** *A*, the level of LDH released from PC12N cells treated at 37 °C for 48 h with supernatant (*sup*) or precipitate (*ppt*) obtained by ultracentrifuging (540,000 × *g*, 15 min) incubation mixtures (*whole*) containing Arctic-type Aβ (*Aβ40*) at final concentration of 25 μM, which had been preincubated at 50 μM and 37 °C for 2 h in the absence or presence of 500 μM GM1 ganglioside (the molar ratio of GM1 ganglioside in liposomes was 10%). Each value indicates the percentage level of LDH released following treatment with incubation mixtures relative to the level of LDH released following treatment with Triton X-100. Each *column* indicates the average of three values ± S.D. *, $p < 0.0001$. *B*, dot blot analysis of supernatant (*sup*) obtained by ultracentrifuging incubation mixtures (*whole*) containing Arctic-type Aβ alone, GM1 ganglioside alone, or Arctic-type Aβ plus GM1 ganglioside. The blots were reacted with anti-Oligo (BIOSOURCE Inc., Camarillo, CA) or cholera toxin subunit B-horseradish peroxidase conjugate (Sigma) (*CTX*). *C*, the level of LDH released from PC12N cells and primary neurons treated at 37 °C for 48 h with incubation mixtures containing Arctic-type Aβ (Aβ40) at a final concentration of 25 μM, which had been preincubated at 50 μM and 37 °C for 2 h in the presence of GM1 ganglioside and anti-Oligo. Each *column* indicates the average of three values ± S.D. *, $p < 0.0001$. *D*, the level of LDH released from PC12N cells treated at 37 °C for 48 h with Arctic-type Aβ, which had been preincubated in the presence of GM1 ganglioside and 4396C. Each column indicates the average of three values ± S.D. *n.s.*, not significant.

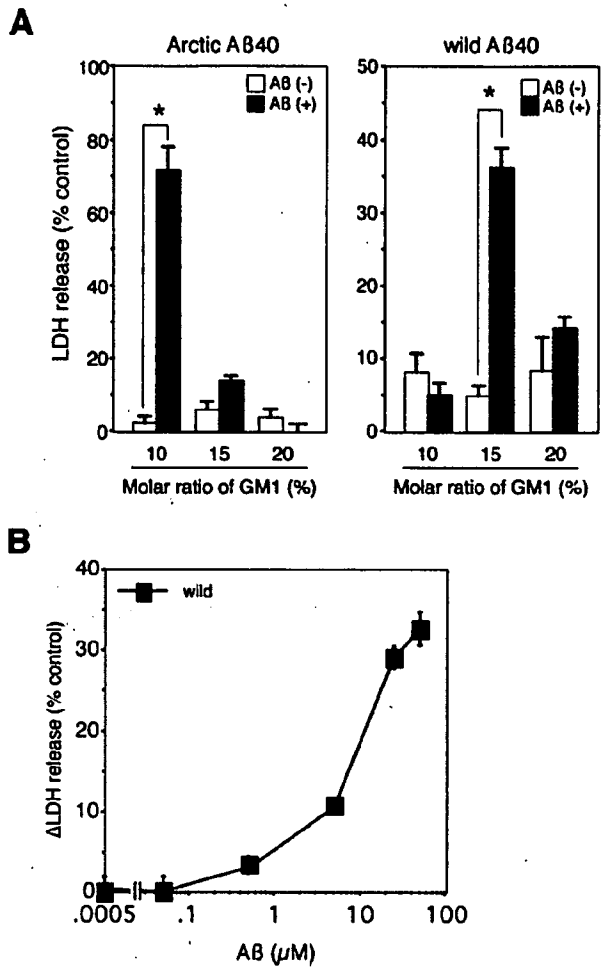

FIGURE 3. **TAβ formation from wild-type Aβ.** *A*, the level of LDH released from NGF-treated PC12 (PC12N) cells treated at 37 °C for 48 h with incubation mixtures containing Arctic-type Aβ (Aβ40), wild-type Aβ (Aβ40) at a final concentration of 25 μM, which had been preincubated at 50 μM for 2 h at 37 °C in the presence of GM1-ganglioside-containing liposomes. The GM1 ganglioside concentration in the incubation mixtures was 500 μM, and the molar ratio of GM1 ganglioside in liposomes varied as indicated. Each value indicates the percentage level of LDH released following treatment with incubation mixtures relative to the level of LDH released following treatment with Triton X-100. Each column indicates the average of three values ± S.D. *, $p < 0.0001$. *B*, the level of LDH released from PC12N cells treated at 37 °C for 48 h with incubation mixtures containing wild-type Aβ at various concentrations, which had been preincubated in the absence or presence of 500 μM GM1 ganglioside (the molar ratio of GM1 ganglioside in liposomes was 15%). Each point indicates the LDH level in the incubation mixtures containing GM1 ganglioside minus that of the incubation mixtures lacking GM1 gangliosides, which was negligible below 25 μM for wild-type Aβ.

Putative Mechanism Underlying TAβ-induced Neuronal Death—To characterize cell death induced by TAβ, we performed nuclear staining with a membrane-permeable dye, Hoechst 33258. PC12N cells, which were treated with incubation mixtures containing TAβ for 12 h, showed characteristics of apoptotic changes, including retracted neurites, shrunken

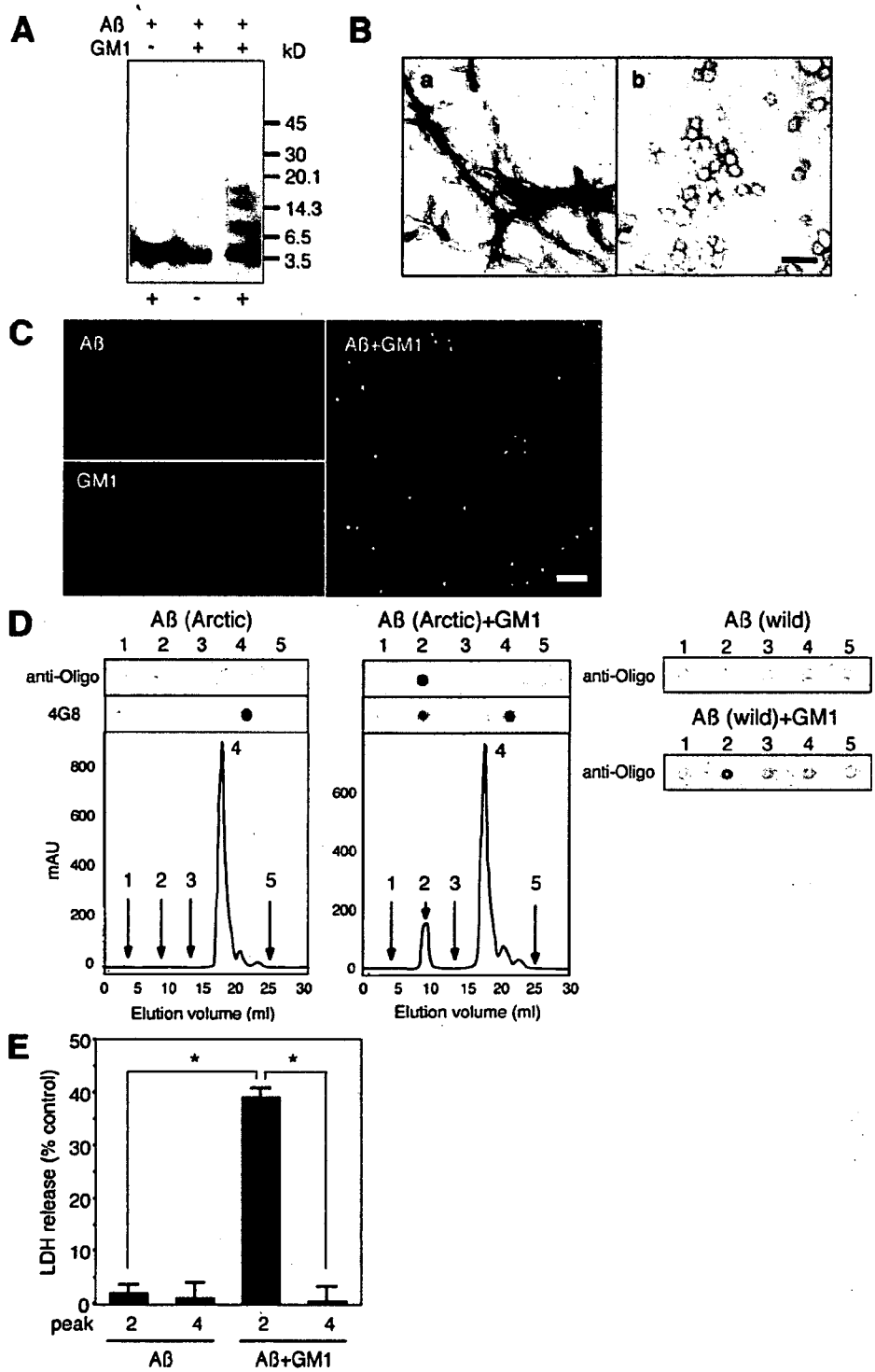

FIGURE 4. **Biophysical and structural analyses of TAβ.** *A*, Western blot of supernatants of incubation mixtures containing Arctic-type Aβ (Aβ40), which had been incubated at 50 μM and 37 °C for 24 h in the absence or presence of 500 μM GM1 ganglioside (the molar ratio of GM1 ganglioside in liposomes was 10%). Ten nanograms of Aβ in the incubation mixtures was subjected to SDS-PAGE (4–20% gradient gel) with (+) or without (−) cross-linking pretreatment using glutaraldehyde. The blot was reacted with 4G8. *B*, electron micrographs of incubation mixture containing Arctic-type Aβ preincubated to allow protofibril formation (*a*) or of incubation mixture containing TAβ formed from Arctic-type Aβ (*b*). Typical protofibril structures were observed in *a*; however, no definite structures aside from liposomes were observed in *b*. *Bar*, 100 nm. *C*, AFM image of fraction containing TAβ formed from Arctic-type Aβ. The supernatant obtained by ultracentrifuging (540,000 × *g*, 3 h) the incubation mixture containing TAβ was subjected to AFM. Spherical particles along with rod-shaped structures were observed. No definite structures were observed in the supernatants of incubation mixtures containing Arctic-type Aβ alone or GM1 ganglioside alone. The amplitude range is 0.1 V. *Bar*, 200 nm. *D*, size exclusion chromatography of incubation mixtures containing Aβ, which had been preincubated in the absence or presence of GM1 ganglioside, on a Superose 12 column. Elution samples from 35 fractions were dot-blotted on nitrocellulose membranes. The blot was reacted with anti-Oligo or 4G8. The immunoreactivity with anti-Oligo was recovered as a single peak with an apparent molecular mass of 200–300 kDa. Five representative fractions are shown. *Peaks 2* and *4* correspond to fractions containing TAβ and monomeric Aβ, respectively. *mAU*, milli-absorbance unit. *E*, toxicities of peaks (*2* and *4*) collected from incubation mixtures containing Arctic-type Aβ (shown in *D*) against PC12N cells. Each *column* indicates the average of three values ± S.D.*, $p < 0.0001$.